

## ABSTRACT

CRAWFORD, KAITLYN ELYSE. Growth and Degradation of Poly(glycolic acid) and Poly( $\epsilon$ -caprolactone) Brushes. (Under the direction of Christopher B. Gorman).

In this work the surface-initiated ring-opening polymerization (SI-ROP) of glycolide and  $\epsilon$ -caprolactone was studied. Surface silanol groups on silicon were used as initiators and tin(II) 2-ethylhexanoate ( $\text{Sn}(\text{Oct})_2$ ) was used as a catalyst. The resulting poly(glycolic acid) (PGA) and poly( $\epsilon$ -caprolactone) (PCL) brushes were grown using the standardized procedures set forth by previous group member, Dr. Lebo Xu, for poly(lactic acid) (PLA) brushes. The original parameters used for PLA brushes were successfully applied for PGA brush growth. However, further adjustments to the original parameters were made for PGA brushes in an effort to optimize brush growth in the plane perpendicular to the silicon surface. It was found that PCL brush growth was less predictable than for PGA or PLA brushes and that PGA brushes grew better at ambient temperatures. The characterization techniques employed were ellipsometry, attenuated total reflectance Fourier transform infrared spectroscopy (ATR-FTIR) and deionized water contact angle measurements.

Preliminary work on the degradation of PGA and PCL brushes was also completed. Polyester brush degradation was carried out in phosphate buffer solutions at low and high pH at 37 °C. Changes in brush thickness were tracked *via* ellipsometry and plotted as a function of time. The results indicate that PCL brushes degrade more slowly than PGA brushes and that the relative rates of degradation for both PCL and PGA brushes increase with increasing pH.

Growth and Degradation of Poly(glycolic acid) and Poly( $\epsilon$ -caprolactone) Brushes

by  
Kaitlyn Elyse Crawford

A thesis submitted to the Graduate Faculty of  
North Carolina State University  
in partial fulfillment of the  
requirements for the Degree of  
Master of Science

Chemistry

Raleigh, North Carolina

2011

APPROVED BY:

---

Christopher B. Gorman  
Chair of the Advisory Committee

---

Jan Genzer

---

Edmond F. Bowden

---

Walter Weare

## BIOGRAPHY

Kaitlyn Crawford graduated from the University of North Carolina at Charlotte in 2009 with a B.S. in Chemistry and Psychology. During her undergraduate studies, Kaitlyn worked under the advisement of Professor Sherine O. Obare for research on the synthesis of Palladium and Ruthenium bimetallic nanoparticles for use in catalysis. The nanoparticles were synthesized in both homogeneous and heterogeneous form. Kaitlyn received four awards for her outstanding research in this area. (1) *The Carolina Chemistry Club Research Award* (February 2009), (2) *The 237<sup>th</sup> National Meeting of the American Chemical Society Colloid and Surface Materials Section Poster Winner* (March 2009), (3) *The Carolina Chemistry, American Chemical Society, Piedmont Section Research award* (April 2009) and (4) *2<sup>nd</sup> place in the Undergraduate Research Conference Oral Presentation Contest hosted by the University of North Carolina at Charlotte* (April 2009).

Kaitlyn entered the graduate program at North Carolina State University in 2009. During her graduate studies Kaitlyn worked under the guidance of Professor Christopher B. Gorman. She studied the growth of biodegradable polyester brushes composed of poly(glycolic acid) and poly( $\epsilon$ -caprolactone). While working on her master's degree at North Carolina State University, Kaitlyn taught general chemistry labs and received the *Dennis Wertz Excellence of Teaching Award* (March 2010). She is a co-author in the recently published *Macromolecules* article on the degradation of poly(lactic acid) brushes (June 2011).

## TABLE OF CONTENTS

<b>List of Figures</b> .....	v
------------------------------	---

<b>List of Schemes</b> .....	viii
------------------------------	------

<b>Chapter 1: Introduction</b> .....	1
1.1. Impetus .....	1
1.2. Background for Bulk Poly(glycolic acid) and Poly( $\epsilon$ -caprolactone) .....	1
1.3. Background for Poly(glycolic acid) and Poly( $\epsilon$ -caprolactone) as Polymer Brushes .....	7
1.3.1. Definition for poly(glycolic acid) and poly( $\epsilon$ -caprolactone) as polymer brushes .....	7
1.3.2. Synthesis of grafted polymer chains .....	8
1.3.3. Polymer brush morphology .....	10
1.3.4. Stimuli-responsive brushes .....	11
1.3.5. Poly(lactic acid) and poly( $\epsilon$ -caprolactone) brushes .....	12
1.3.6. Ellipsometry used to measure polymer brush thickness .....	13
1.4. Conclusion .....	15
1.5. References .....	15

<b>Chapter 2: Application of Standardized Polymer Brush Growth Conditions for Poly(lactic acid) to the Growth of Poly(glycolic acid) and Poly(<math>\epsilon</math>-caprolactone) Brushes</b> .....	22
2.1. Introduction .....	22
2.1.1. Optimal growth conditions previously determined for poly(lactic acid) brushes .....	22
2.2. Results and Discussion .....	25
2.2.1. Reproducing Poly(lactic acid) brush growth .....	25
2.2.2. Poly(glycolic acid) brush growth .....	30
2.2.3. Poly( $\epsilon$ -caprolactone) brush growth .....	34
2.3. Conclusion .....	37
2.4. Experimental Details .....	37
2.4.1. Si chip preparation .....	37
2.4.2. Polymer brush growth preparation .....	38
2.4.3. Reaction quenching .....	38
2.4.4. Distilled or recrystallized monomers and solvents .....	39
2.4.5. Instrumentation methods .....	40
2.4.5.1. Ellipsometry .....	40
2.4.5.2. ATR-FTIR .....	40

2.4.5.3. DI water contact angle .....	40
2.4.6. Glassware .....	41
2.5. References .....	41

### **Chapter 3: Adjustments to Standardized Polymer Brush growth**

#### **Conditions to Maximize the Thickness of the Poly(glycolic acid) Brushes ..43**

3.1. Introduction .....	43
3.1.1. Changes to standard conditions .....	43
3.3. Results and Discussion .....	44
3.3.1. Effects of temperature .....	44
3.3.2. Effects of static vs. non-static growth environments .....	46
3.3.3. Experimental techniques .....	48
3.3.3.2. Polymer brush preparation techniques .....	51
3.3.4. Glycolide purification .....	54
3.4. Conclusion .....	57
3.5. Experimental Details .....	57
3.5.1. Si chip preparation .....	57
3.5.2. Polymer brush growth preparation .....	58
3.5.3. Reaction quenching .....	58
3.5.4. Distilled or recrystallized monomers and solvents .....	59
3.5.5. Ellipsometry .....	59
3.5.6. Glassware .....	60
3.6. References .....	60

### **Chapter 4: Poly(glycolic acid) and Poly( $\epsilon$ -caprolactone) Brush**

#### **Degradation: Preliminary Results .....**

4.1. Introduction .....	61
4.2. Results and Discussion .....	68
4.2.1. Reproducing poly(lactic acid) brush degradation .....	68
4.2.2. Poly(glycolic acid) brush degradation .....	69
4.2.3. Poly( $\epsilon$ -caprolactone) brush degradation .....	71
4.3. Conclusion .....	73
4.4. Proposal for Future Work .....	74
4.5. Experimental Details .....	76
4.5.1. Polymer brush degradation .....	76
4.5.2. Ellipsometry .....	76
4.5.3. Glassware .....	76
4.6. References .....	77

## LIST OF FIGURES

Figure 1.1:	Representation of grafted polymers with different morphologies. Fully extended (left), partially collapsed (middle) and fully collapsed state (right). <sup>35</sup>	10
Figure 1.2:	Transition from the mushroom regime to the brush regime reported for polyacrylamide brushes reported by Genzer and coworkers. <sup>47</sup>	11
Figure 1.3:	Schematic representation of an ellipsometer. <sup>62</sup>	14
Figure 2.4:	Plots of ellipsometric thicknesses vs. growth time at different temperatures. Reaction conditions: [L-lactide] = 0.1 M, [Sn(Oct)2] = 0.001 M, 24 h. Error bars represent the magnitude of the 90% confidence interval for five measurements on a single sample. This data was completed by Dr. Lebo Xu has been reproduced here for exemplary purposes.	24
Figure 2.5:	Plots of ellipsometric thicknesses of PLA brushes versus growth time. Plots represent the result of PLA brushes synthesized with water contaminated THF (black squares) and impure monomer (blue circles). Reaction conditions: [L-lactide] = 0.1 M, [Sn(Oct)2] = 0.001 M, 19 °C. Error bars represent the magnitude of the 90% confidence interval for 10 measurements across two samples.	26
Figure 2.6:	Plots of ellipsometric thicknesses of PLA brushes versus growth time. Plots represent the result of PLA brushes synthesized in dry solvent with pure monomer. Reaction conditions: high purity [L-lactide] = 0.1 M, [Sn(Oct)2] = 0.001 M, 19 °C. Error bars represent the magnitude of the 90% confidence interval for 10 measurements across two samples.	27
Figure 2.7:	Plots of ellipsometric thicknesses of PLA brushes versus growth time. Reaction conditions: high purity [L-lactide] = 0.1 M, [Sn(Oct)2] = 0.001 M. Red circles are published data from Xu, ca. 25 °C. Black squares represent the reproducibility of Xu's work, 28 °C. Error bars represent the magnitude of the 90% confidence interval for 10 measurements across two samples.	28
Figure 2.8:	DI water contact angle measurements on PLA brush samples with increasing ellipsometric thickness.	29
Figure 2.9:	ATR-FTIR of PLA Brush sample with ca. 100 Å ellipsometric thickness.	30

Figure 2.10:	Plots of ellipsometric thicknesses of PLA brushes versus growth time. Reaction conditions: [glycolide] = 0.1 M, [Sn(Oct) <sub>2</sub> ] = 0.001 M, 28 °C. Error bars represent the magnitude of the 90% confidence interval for 10 measurements across two samples.....	31
Figure 2.11:	DI water contact angle measurements on PGA brush samples with increasing ellipsometric thickness.....	32
Figure 2.12:	ATR-FTIR of PGA Brush sample with ca. 100 Å ellipsometric thickness.....	33
Figure 2.13:	Plots of ellipsometric thicknesses of PLA brushes versus growth time. Plots show the irreproducibility of PCL brushes under the same reaction conditions: [ε-caprolactone] = 0.1 M, [Sn(Oct) <sub>2</sub> ] = 0.001 M, ca. 25 °C. Error bars represent the magnitude of the 90% confidence interval for 10 measurements across two samples.....	34
Figure 2.14:	DI water contact angle measurements on PCL brush samples with increasing ellipsometric thickness.....	35
Figure 2.15:	ATR-FTIR of PCL Brush sample with ca. 100 Å ellipsometric thickness.....	36
Figure 3.16:	(Left) Plots of ellipsometric thickness vs. growth time for PGA brushes at 8, 28, 37 and 60 °C. Reaction conditions: [glycolide] = 0.1 M, [Sn(Oct) <sub>2</sub> ] = 0.001 M, sample rotation speed = 100 RPM. Error bars represent the magnitude of the 90% confidence interval for 10 measurements across two samples. (Right) Optical images of reaction vessels after 24 h of reaction time at ambient (above) and elevated (below) temperatures. ....	46
Figure 3.17:	Plots of ellipsometric thickness vs. growth time for PGA brushes at 0, 100 and 300 RPM rotation speeds. Reaction conditions: [glycolide] = 0.1 M, [Sn(Oct) <sub>2</sub> ] = 0.001 M, 28 °C. Error bars represent the magnitude of the 90% confidence interval for 10 measurements across two samples. ....	47
Figure 3.18:	Histogram of ellipsometric thickness vs. growth time for PGA brushes after 24 h of reaction time. Reaction conditions: [glycolide] = 0.1 M, [Sn(Oct) <sub>2</sub> ] = 0.001 M, sample rotation speed = 100 RPM, 28 °C. Error bars represent the magnitude of the 90% confidence interval for 10 measurements across two samples.....	50

- Figure 3.19: Histogram of ellipsometric thickness vs. growth time for PGA brushes after 24 h of reaction time. Data points represent six separate sample preparation methods: (1) No catalyst, (2) No catalyst but addition of H<sub>2</sub>O on sample surface, (3) 15  $\mu$ L catalyst (0.001 M) on sample surface followed by 15  $\mu$ L H<sub>2</sub>O after addition of monomer, (4) “Control” sample, 15  $\mu$ L catalyst (0.001 M) on sample surface, (5) 15  $\mu$ L catalyst (0.001 M) added after monomer and (6) 60  $\mu$ L catalyst (0.006 M) on sample surface. Remaining reaction conditions: [glycolide] = 0.1 M (5 mL aliquot for each sample), sample rotation speed = 100 RPM, 28 °C. Error bars represent the magnitude of the 90% confidence interval for 10 measurements across two samples.....52
- Figure 3.20: Histogram of ellipsometric thickness vs. growth time for PGA brushes after 24 h of reaction time. Reaction conditions: [glycolide] = 0.1 M, [Sn(Oct)<sub>2</sub>] = 0.001 M, sample rotation speed = 100 RPM, 28 °C. Error bars represent the magnitude of the 90% confidence interval for 10 measurements across two samples.....54
- Figure 3.21: Histogram of ellipsometric thickness vs. growth time for PGA brushes after 24 hours of reaction time for brushes grown using glycolide recrystallized from different solvents. Trial 1: toluene only (twice recrystallized); trial 2: ethyl acetate followed by acetone; trail 3: ethyl acetate only (twice recrystallized); trial 4: ethyl acetate followed by acetonitrile. All solvents were anhydrous. Reaction conditions: [glycolide] = 0.1 M, [Sn(Oct)<sub>2</sub>] = 0.001 M, sample rotation speed = 100 RPM, 28 °C. Error bars represent the magnitude of the 90% confidence interval for 10 measurements across two samples.....55
- Figure 4.22: Plots of ellipsometric thicknesses versus degradation time at different temperatures. Phosphate buffer pH = 7.4 with 10 mM ionic strength used to control pH. Error bars represent the magnitude of the 90% confidence interval for 5 measurements on a sample.....65
- Figure 4.23: Plots of ellipsometric thicknesses versus degradation time at 37 °C with different pH values. Phosphate buffers of 10 mM ionic strength were used to control pH. Error bars represent the magnitude of the 90% confidence interval for 5 measurements on a sample.....66
- Figure 4.24: Plots of ellipsometric thicknesses versus degradation time for PLA brushes. Reaction conditions: phosphate buffer (10 mM ionic strength), pH 7.4 at 37 °C. Error bars represent the magnitude of the 90% confidence interval for 5 measurements on a sample.....69

Figure 4.25: Plots of ellipsometric thicknesses versus degradation time comparing a PGA and PLA brush. Reaction conditions: phosphate buffer (10 mM ionic strength), pH 7.4 at 37 °C. Error bars represent the magnitude of the 90% confidence interval for 5 measurements on a sample. ....70

Figure 4.26: Plots of ellipsometric thicknesses versus degradation time for PCL brushes. Reaction conditions: phosphate buffer (10 mM ionic strength), 37 °C, changed sample solution daily after ca. 110 h. Error bars represent the magnitude of the 90% confidence interval for 5 measurements on a sample. ....72

## LIST OF SCHEMES

Scheme 1.1: ROP of glycolide.....	2
Scheme 1.2: ROP of $\epsilon$ -caprolactone.....	3
Scheme 1.3: Two step ROP of lactide with Sn(II)Oct <sub>2</sub> .....	5
Scheme 4.4: Proposed random chain scission mechanism for hydrolysis of PGA (A) and PCL (B).....	62
Scheme 4.5: Proposed backbiting mechanism for the hydrolysis of PGA (A) and PCL (B).....	63
Scheme 4.6: Molecular structures of glycolide, lactide and $\epsilon$ -caprolactone. ....	68

# Chapter 1: Introduction

## 1.1. Impetus

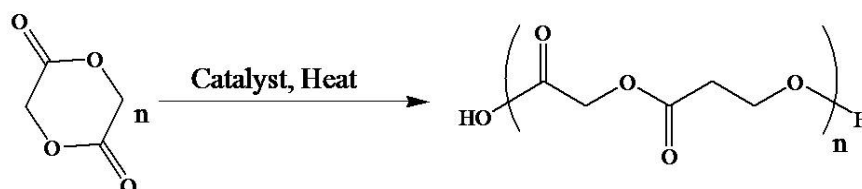
Polyesters such as poly(glycolic acid) (PGA) and poly( $\epsilon$ -caprolactone) (PCL) have been of particular interest for both biomedical and environmental applications due to their biodegradability and low toxicity.<sup>1</sup> This chapter is an overview of how PGA and PCL became of interest, including the types of applications PGA and PCL have been used for and their potential use as polymer brushes. The aim of subsequent chapters is to establish homopolymer brush growth for PGA and PCL and to briefly review their biodegradability in phosphate buffer solutions.

## 1.2. Background for Bulk Poly(glycolic acid) and Poly( $\epsilon$ -caprolactone)

Poly(glycolic acid) (PGA) can be synthesized from glycolic acid or glycolide monomer and was first discovered in 1954.<sup>2</sup> As a result of this discovery, two methods of polymerization for PGA were realized. The first was through the polycondensation of glycolic acid. The second was through ring-opening polymerization (ROP) of the cyclic diester of glycolic acid commonly known as glycolide (Scheme 1.1). The monomer components can be obtained from renewable resources such as sugar cane.<sup>3</sup> As a homopolymer PGA is fibrous and has had limited use due to its hydrolytic instability.<sup>4</sup> The most commonly used application for PGA is surgical sutures.<sup>4</sup> However, when PGA is

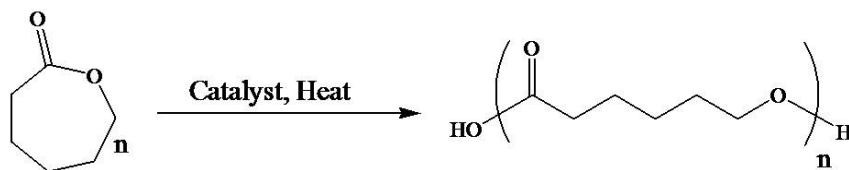
combined with other polymers in co-block or random form the number of potential biomedical and environmental applications is greatly increased.

Scheme 1.1: ROP of glycolide.



Poly( $\epsilon$ -caprolactone) (PCL) was first synthesized from  $\epsilon$ -caprolactone by Van Natta in 1934.<sup>5</sup> The most widely used mechanism for the polymerization of  $\epsilon$ -caprolactone is through ROP. This method yields PCL with a high molecular weight and low monodispersity (Scheme 1.2).<sup>6</sup> PCL can also be synthesized through the polycondensation of 6-hydroxyhexanoic acid; however, this approach is employed less frequently than ROP because it is less effective for the production of high molecular weight polymer with low monodispersity. For ROP, the  $\epsilon$ -caprolactone monomer can be produced from natural resources; however synthesis methods from natural resources are expensive and are not used regularly. Instead,  $\epsilon$ -caprolactone is most commonly extracted from crude oil.<sup>7</sup> PCL displays a unique property in that it is miscible in other polymers such as poly(vinyl chloride) and polycarbonates.<sup>6</sup>

Scheme 1.2: ROP of  $\epsilon$ -caprolactone.



The use of PGA and PCL in homopolymer, co-block or random polymer form has facilitated enormous advancements in the biomedical field due largely to their biocompatible and biodegradable properties. When combined with each other or with other polymers such as poly(ethylene oxide) (PEG) or poly(lactic acid) (PLA) numerous applications have surfaced, such as, sutures,<sup>8</sup> stents, drug delivery vehicles,<sup>9</sup> surgical screws and prosthetics.<sup>10</sup> PGA and PCL have also been studied for ocular and oral applications such as contact lenses<sup>11</sup> and dental implants.<sup>4</sup>

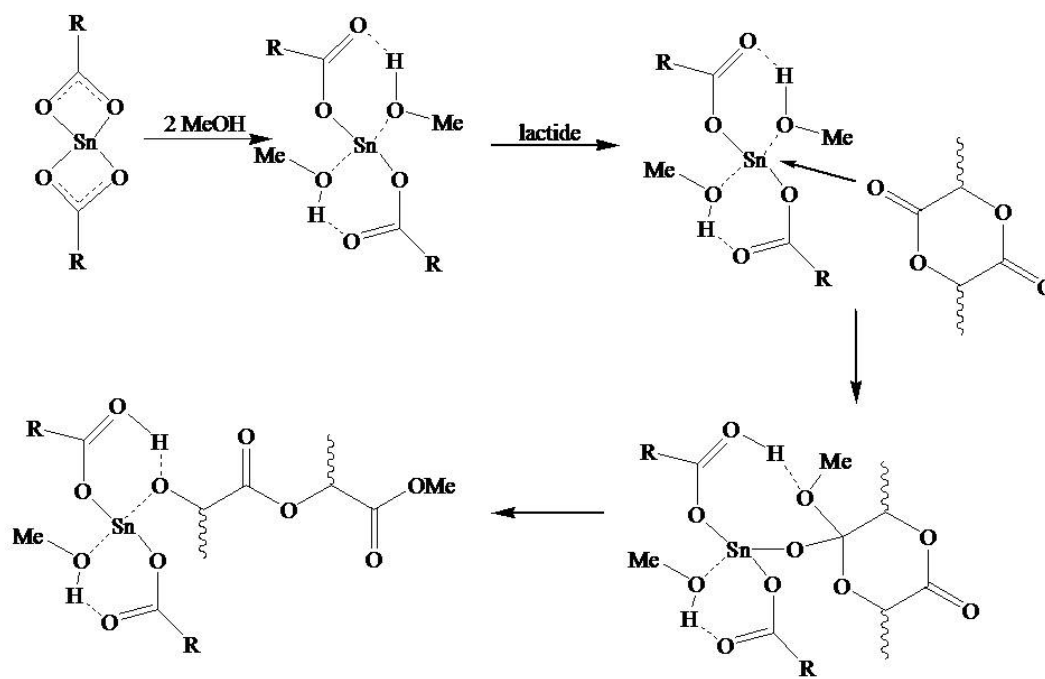
Though ROP is the primary synthesis method used for PGA, PCL, the individual components involved may be quite different depending on the application of interest. Based on the type of catalyst or the reaction environment (temperature, pressure etc) employed for ROP the resulting polyesters will display very different properties such as changes in molecular weight, monodispersity, crystallinity, hydrophobicity and tensile strength.<sup>10,12</sup> Since different applications require different polymeric properties, all of the aforementioned polymer characteristics play a significant role when choosing the necessary components involved for polymerization. For example, the ROP of PCL carried out at elevated temperatures (140-180 °C) using  $\text{Sn}(\text{Oct})_2$  as a catalyst is fast, with polymerization occurring

after only a few minutes or after a few hours. Whereas the use aluminum isopropoxide ( $\text{Al}(\text{Oi-Pr})_3$ ) as a catalyst instead of  $\text{Sn}(\text{Oct})_2$  under similar conditions can take several days for polymerization. As a result a more narrow molecular weight is obtained from ROP polymerization with the catalyst  $\text{Sn}(\text{Oct})_2$  as opposed to  $\text{Al}(\text{Oi-Pr})_3$ .<sup>13,14</sup> Furthermore, PCL fibers studied for bone fixation were manipulated by melting which resulted in a thread like product with greater strength than a stainless-steel wire with the same cross-sectional area.<sup>15</sup> When PGA is blended with polyethylene terephthalate (PET), known as Kuredux<sup>®</sup>, the resulting polymer can succumb to degradation more easily and has thus been applied to products such as disposable plastic cups, utensils and grocery bags.<sup>16</sup>

When considering the ROP of PGA and PCL, the most widely used catalyst is tin (II) 2-ethylhexanoate ( $\text{Sn}(\text{Oct})_2$ ).  $\text{Sn}(\text{Oct})_2$  is a highly active catalyst and is U.S. FDA approved. Despite its wide spread use, controversy still exists regarding the mechanism by which polymerization occurs.<sup>6</sup> The general consensus is that ROP occurs through a coordination-insertion mechanism with the help of a protic solvent.<sup>13,17</sup> The exact mechanism that occurs is still being debated, however. When using a protic solvent (i.e. an alcohol)  $\text{Sn}(\text{Oct})_2$  can form tin alkoxides. What happens next is the primary source of concern. Once the tin alkoxide has formed it is unclear whether the octoate ligands remain coordinated with the tin or are released from coordination, or both. A recent computational study for the methanol assisted ROP of PLA using  $\text{Sn}(\text{Oct})_2$  suggests a two step mechanism (Scheme 1.3). The first step consists of methanol coordination with the tin forming an alkoxide. The second step involves coordination with the lactide monomer resulting in ring-opening and thus

allowing for further polymerization to continue in a living fashion.<sup>17</sup> Although, the mechanism has been reported for PLA, the mechanism can likely be applied to PGA and PCL.<sup>18</sup>

Scheme 1.3: Two step ROP of lactide with Sn(II)Oct<sub>2</sub>.<sup>19</sup>



When considering PGA and PCL for biodegradation it has been shown that the rate of

degradation is dependent on both, the properties of the polymer (e.g. molecular weight and crystallinity), and the environment to which the polymer is exposed.<sup>20</sup> Takiyama reported that aliphatic polyesters show a decrease in degradability when the molecular weight is above 50,000.<sup>21</sup> Albertsson and Varma showed that biodegradation occurs more rapidly from the amorphous, as opposed to crystalline, regions of polyesters.<sup>22,23</sup> Thus, the crystallinity of the polyester is increased during degradation.<sup>22,24</sup>

As indicated, the study of lactone based polyesters has been paramount toward the advancement of biomedical and environmental applications. Moreover, the polymerization methods employed can be individually tailored to fit the application of interest. Adjustments to polymer synthesis may include changes to the monomer (e.g. type and concentration) or to the reaction environment (e.g. temperature, catalyst, pH, solvent). It is important to understand how variations made to the polymerization method will affect the end product. For example, if a polymer is too crystalline, it may take too long to degrade or if the polymers' structure is too amorphous it may degrade too quickly.<sup>25</sup> All of these factors need to be considered.

### **1.3. Background for Poly(glycolic acid) and Poly( $\epsilon$ -caprolactone) as Polymer Brushes**

#### **1.3.1. Definition for poly(glycolic acid) and poly( $\epsilon$ -caprolactone) as polymer brushes**

While PGA and PCL have been studied extensively in bulk form, there is a lack of literature that explains the behavior of PGA and PCL on a molecular scale. More specifically, the investigation of the standardized growth and the relative rates of degradation for homopolymer brushes composed of PGA and PCL are a largely uncharted area. Polymer brushes have gained increasing attention over the years for their use in applications that involve adhesion,<sup>26,27</sup> lubrication,<sup>28</sup> protective coatings,<sup>29,30</sup> adsorption<sup>31</sup> and microelectronics.<sup>32,33</sup> A polymer brush is a type of thin film that is composed of a group of polymers where one polymer chain end is anchored to a surface and the other end of the polymer chain (the terminal end) is free from surface tethering.<sup>34</sup> Polymer brushes display some unique properties compared to their bulk polymer counterparts. The most unique property observed with polymer brushes is their structural deformity. Due to the structural confinement of the polymer as a brush, the individual polymer chains orient themselves so as to reduce the amount of free energy of interaction per chain (resulting in structural deformity). However, as the polymer chains elongate away from the tethered surface, reducing the interaction energy, there is a subsequent increase in the elastic free energy. This theory stems from the Alexander model (Eq. 1).<sup>35,36,37</sup>

$$F = F_{\text{int}} + F_{\text{el}} \quad \text{Eq. 1}$$

In Eq. 1,  $F$  is the free energy of the polymer brush which is equal to the sum of the interaction free energy and the elastic free energy,  $F_{\text{int}}$  and  $F_{\text{el}}$  respectively. The Alexander model is one of the simplest mathematical models for determining the free energy of the brush.<sup>35</sup> This model is only an approximation, however and is completely valid only under the following 3 constraints. First the polymer chains must be monodisperse and tethered to a nonadsorbing flat surface. Second there must be a constant concentration of polymer chains. Third the free, untethered chain ends must all be located on the same plane at a given distance from the surface.<sup>35</sup> Although Alexander was one of the first scientists to define polymer brushes in this way, the synthesis of polymer brushes had been suggested since before the 1950s.<sup>34</sup> The tools for proper polymer brush characterization were not available until the early 1950s, however.<sup>38,39</sup>

### **1.3.2. Synthesis of grafted polymer chains**

There are two approaches to polymer brush synthesis. The first is through the reversible physisorption of polymer chains on the surface. The second is through covalent bonding between the polymer chains and the grafting surface. The latter approach is considered irreversible due to the stable nature of the covalent bond.<sup>35</sup> In contrast, the stability of polymer chains tethered to the surface via physisorption depends a great deal on the environment that the brushes are exposed to i.e. temperature and solvent.

Ideally, physisorbed polymer brushes would be made with a co-block polymer in which one portion of the polymer chain is more attracted to the surface than the solvent while

the other portion of the polymer chain is more strongly attracted to the solvent than the surface.<sup>40</sup> For example, Parsonage et al. reported diblock polymer brushes of poly(vinylpyridine) (PVP) and polystyrene (PS) on silicon (or mica) surfaces in toluene. The PVP portion of the polymer chain is partially insoluble in toluene and thus adsorbs on the surface. The PS portion of the polymer chain is highly soluble in toluene and thus extends into the solvent maximizing the contact between the solvent and the PS chain.<sup>35,41</sup> Polymer brushes formed from physisorption are less robust. The brushes are hindered by the chains' susceptibility to desorb from the surface upon changes made to the surrounding temperature or solvent.

The polymer brushes formed from covalent bonding are made from two different methods: "grafting to" the surface and "grafting from" the surface. The grafting to method involves the use of polymers that have already been synthesized. The pre-made polymers are grafted to the surface of the substrate of interest. The grafting to method allows for easy control over the molecular weight of the polymer chains. However, the grafting to method is used less frequently due to inherently lower and less predictable grafting densities.<sup>35</sup>

The grafting from approach involves polymer growth that is initiated at the surface. Once initiated, propagation of the polymer chain continues until a means of termination occurs. Termination can occur from the complete conversion of monomer or through reaction quenching. Polymerization can also cease if a thermodynamic equilibrium has been established.<sup>42</sup>

### 1.3.3. Polymer brush morphology

The morphology of a polymer brush is an important factor to consider and can change depending on the grafting density or the environment that the brush is exposed to (solvent polarity, pH, temperature etc.). The grafting density is defined as the number of polymer chains per square area. Based on the grafting density and the surrounding conditions, the polymer brush can be found in one of three states (Figure 1.1). The first is a collapsed form commonly referred to as the mushroom-regime. The collapsed state is caused by a low grafting density or by exposure to an environment that the brush repels (i.e. hydrophobic brush in a hydrophilic solvent). The second morphology is the fully extended form, commonly referred to as the brush-regime. In the brush-regime, the polymer chains are extended in the direction perpendicular to the plane of the surface. This extended brush form results from a high grafting density or by exposing the brush to an attractive environment (i.e. polar brush exposed to a polar solvent). The third morphology is a mixture between the mushroom and brush regime.<sup>32,34,43</sup>



Figure 1.1: Representation of grafted polymers with different morphologies. Fully extended (left), partially collapsed (middle) and fully collapsed state (right).<sup>35</sup>

There are a number of reports that describe how brush morphology changes with grafting density.<sup>44,45,46</sup> For example, Genzer and coworkers created polyacrylamide brushes with a gradient grafting density. The gradient densities were formed by changing the initiator concentration across the surface before polymerization. The brushes were characterized by following the change in brush thickness from one end of the substrate to the other (Figure 1.2).<sup>47</sup> The results of their work and model based calculations they used support the transition from mushroom to brush regime with increasing grafting density.

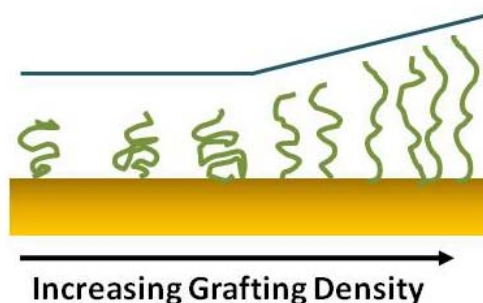


Figure 1.2: Transition from the mushroom regime to the brush regime reported for polyacrylamide brushes reported by Genzer and coworkers.<sup>47</sup>

#### 1.3.4. Stimuli-responsive brushes

The brush morphology that results from changes made to the brush environment is of particular interest for applications that require the activation-inactivation of electrochemical interfaces.<sup>48,49</sup> Thus, in these cases, diffusion control and the control of phase-segregation in response to external stimuli are paramount.<sup>34</sup> Several reports have been made regarding

stimuli responsive surfaces.<sup>50,51,52</sup> Tam et al. reported on how poly(4-vinylpyridine) brushes on an indium-tin oxide surface (ITO) changed morphology from a collapsed to an extended brush form when the pH was increased or decreased respectively.<sup>48</sup> Motornov et al. reported similar findings with poly(2-vinylpyridine)-polyacrylic acid mixed brushes on ITO.<sup>49</sup> Sun et al. demonstrated how changes to temperature effect the surface wettability of poly(N-isopropylacrylamide) brushes on silicon. Variations in surface wettability were tracked by deionized water contact angle measurements. The observed contact angles increased from ca. 63° - 93° upon an increase in temperature (from 25 °C - 40 °C). Thus, a decrease in surface wettability measured by was observed.<sup>53</sup> A computational study by Turgman-Cohen and Genzer showed that, when using controlled radical polymerization, polymer brushes with high grafting density are subject to uneven growth of polymer. The uneven growth is due to the result of the formation of a monomer gradient in solution. Their results show that the phenomenon is exaggerated when using a poor solvent for polymerization.<sup>54</sup>

### **1.3.5. Poly(lactic acid) and poly( $\epsilon$ -caprolactone) brushes**

PLA brushes have been reported previously.<sup>55,56</sup> PLA brushes have also been reported by a previous group member, Dr. Lebo Xu. Xu studied how PLA brush growth would be effected by parameters such as temperature, solvent, concentration and catalyst type. Xu also studied the degradation of PLA brushes and how changes made to the temperature and pH affected the relative rate of degradation. The experimental results suggest that PLA brushes

grow thicker at lower temperatures and degrade more rapidly with increasing pH when exposed to aqueous media.<sup>57</sup>

PCL brushes have been reported previously. However, due to the slow nature of PCL biodegradation, the polymer is most frequently found as a mixed or copolymer brush or brush-like material. Wang and Tan reported PCL brush-like particles grown from a hydroxypropyl cellulose backbone. The water soluble matrix was developed as a potential drug delivery material.<sup>58</sup> Mao and Gan reported the synthesis of copolymer brushes composed of PEG as a hydrophilic polymer backbone with PCL and PGA as the hydrophobic side chains. Mao's report suggests that the smaller micelle-like particles were better for controlled drug loading and release.<sup>59</sup> Zhang and coworkers synthesized two separate toothbrush-like polymers for controlled drug delivery. The first brush-like polymer consisted of a PEG backbone with short branched PCL side chains. The second brush-like polymer was similar to the first except the particle also incorporated poly(2-hydroxyethyl) methacrylate. Zhang reported that the latter brush-like particles performed better as drug carriers than the PEG-PCL brush-like particles alone.<sup>60</sup>

### **1.3.6. Ellipsometry used to measure polymer brush thickness**

Throughout many of the aforementioned literature reports, ellipsometry was the primary technique used to determine the thicknesses of the polymer brushes. Ellipsometry was also the key characterization method applied to the polymer brush work presented in the proceeding chapters. Ellipsometry is an optical technique that can accurately report the

thickness of transparent films on a reflective substrate. The first reported use of ellipsometry was in the late 1800s. However, the technique received little attention until the 1960s when ellipsometry was used on an emerging class of microelectronics.<sup>61</sup> The instrument consists of a monochromatic light source (i.e. He-Ne laser) which reflects off of the substrate and into the detector (Figure 1.3). The detector can differentiate changes in polarized light with great accuracy. For use, the instrument is first calibrated with the known refractive index of the original substrate. Following the application of a transparent film (i.e. a polymer brush) the refractive index of the surface changes. Though small, the changes in reflectivity (i.e. change in polarized light from the incident light source) are easily identified by the detector. The changes detected are then transformed into a surface thickness based on the original calibration parameters that were entered.<sup>62</sup>

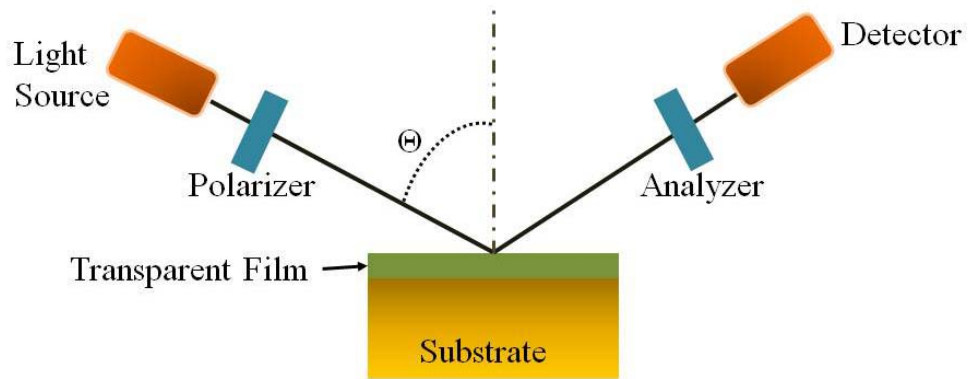


Figure 1.3: Schematic representation of an ellipsometer.<sup>62</sup>

## 1.4. Conclusion

In summary, lactone based polyesters, such as PGA and PCL have been studied a great deal in bulk form for potential use in applications such as, sutures,<sup>8</sup> stents, drug delivery vehicles,<sup>9</sup> surgical screws and prosthetics.<sup>10</sup> Polymer brushes have also been studied a great deal for applications involving adhesion,<sup>26,27</sup> lubrication,<sup>28</sup> protective coatings,<sup>29,30</sup> adsorption<sup>31</sup> and microelectronics.<sup>32,33,31</sup> Based on the biocompatibility and biodegradability of PGA and PCL, it would be interesting to grow PGA and PCL brushes. PGA and PCL as polymer brushes may serve well as temporary protective coatings with potential antibiofouling properties. Thus, the purpose of the work presented in the proceeding chapters will be focused on the reproducible growth of polyester brushes composed of PGA or PCL. Preliminary work on the degradation of these brushes will also be presented.

## 1.5. References

1. Athanasiou, K. A.; Niederauer, G. G.; Agrawal, C. M., Sterilization, Toxicity, Biocompatibility and Clinical Applications of Polylactic acid/polyglycolic acid Copolymers. *Biomaterials* **1996**, *17*, 93-102.
2. Lowe, C. E., Preparation of High Molecular Weight Polyhydroxyacetic Ester. U.S. Patent 2,668,162, Feb 2, 1954.
3. Richardson, K. E.; Tolbert, N. E., Oxidation of Glyoxylic Acid to Oxalic Acid by Glycolic Acid Oxidase. *J. Biol. Chem.* **1961**, *236*, 1280-1284.
4. Gilding, D. K.; Reed, A. M., Biodegradable Polymers for use in Surgery – Polyglycolic/poly(actic acid) homo- and copolymers: 1. *Polymer* **1979**, *20* 1459-1464.

5. Van Natta, F. J.; Hill, J. W.; Carothers, W. H., Studies of Polymerization and Ring Formation. XXIII.  $\epsilon$ -Caprolactone and its Polymers. *The Experimental Station of E. I. Du Pont* **1934**, *118*, 455-457.
6. Lambet, M.; Thielemans, W., Synthesis of Polycaprolactone: a Review. *Chem. Soc. Rev.* **2009**, *38*, 3484-3504.
7. Flieger, M.; Kantorova, M.; Prell, A.; Rezanka, T.; Votruba, J., Biodegradable Plastics from Renewable Sources. *Folia Microbiol.*, **2003**, *1*, 27-44.
8. Pillai, C. K. S.; Sharma, C. P., Review Paper: Absorbable Polymeric Surgical Sutures: Chemistry, Production, Properties, Biodegradability, and Performance. *J. Biomat. App.* **2010**, *25*, 291-376.
9. Kumar, N.; Ravikumar, M. N. V.; Domb, A. J., Biodegradable Block Copolymers. *Adv. Drug Del. Rev.* **2001**, *53*, 23-44.
10. Albertsson, A. C.; Varma, I. K., Recent Developments in Ring Opening Polymerization of lactones for Biomedical Applications. *Biomacromol.* **2003**, *4*, 1466-1486.
11. Ciolino, J. B.; Hoare, T. R.; Iwata, N. G.; Behlau, I.; Dohlman, C. H.; Langer, R.; Kobane, D. S., A Drug-Eluting Contact Lens. *Inves. Ophthal. Vis. Sci.* **2009**, *50*, 3346-3352.
12. Feng, X. D.; Song, C. X.; Chen, W. Y., Synthesis and evaluation of biodegradable block copolymers of  $\epsilon$ -caprolactone and DL-lactide. *J. Polym. Sci. Pol. Lett.* **1983**, *21*, (8), 593-600.
13. Cabaret-Dechy, O.; Martin-Vaca, B.; Bourissou, D., Controlled Ring-Opening Polymerization of Lactide and Glycolide. *Chem. Rev.* **2004**, *104*, 6147-6176.
14. Degee, P.; Dubois, P. H.; Jerome, R.; Jacobsen, S.; Fritzh, G., New Catalysis for Fast Bulk Ring-Opening Polymerization of Lactide Monomers. *Macromol. Symp.* **1999**, *144*, 289-302.
15. Hattori, K.; Tomita, N.; Woshikawa, T.; Takakura, Y., Prospects for Bone Fixation – Development of New Cerclage Fixation Techniques. *Mat. Sci. Eng.* **2001**, *17*, 27-32.

16. Kureha Home Page. <http://kureha.com> (accessed June 2011).
17. Kricheldorf, H.; Kreiser-Saunders, I.; Stricker, A., Poly lactones 48. SnOct<sub>2</sub>-Initiated Polymerizations of Lactide: A Mechanistic Study. *Macromol.* **2000**, *33*, 702-709.
18. In't Veld, P. J. A.; Velner, E. M.; Van de Witte, P. Hamhius, J.; Dijkstra, P. J.; Feijen, J., Melt Block Copolymerization of  $\epsilon$ -Caprolactone and L-lactide. *J. Polym. Sci.: Part A: Polym. Chem.* **1997**, *35*, 216-226.
19. Ryner, M.; Stridsberg, K.; Albertsson, A. C.; von Schenck, H.; Svensson, M., Mechanism of Ring-Opening Polymerization of 1,5-Dioxepan-2-one and L-Lactide with Stannous 2-Ethylhexanoate. A Theoretical Study. *Macromol.* **2001**, *34*, 3877-3881.
20. Albertsson, A. C.; Varma, I. K., Aliphatic Polyesters: Synthesis, Properties and Applications. *Adv. Polym. Sci.* **2002**, *157*, 1-40.
21. Takiyama, E.; Fujimaki, T., Characteristics of biodegradable aliphatic polymer - bionolle. *Plastics* **1992**, *43*, 87.
22. Albertsson, A. C.; Varma, I. K., Aliphatic Polyesters: Synthesis, Properties and Applications. *Adv. Polym. Sci.* **2002**, *157*, 1-40.
23. Li, S., Hydrolytic Degradation Characteristics of Aliphatic Polyesters Derived from Lactic and Glycolic Acids. *J. Biomed. Mater. Res.* **1999**, *48*, 342-353.
24. Zurita, R.; Franco, L.; Puiggali, J.; Rodriguez-Galan, A., They Hydrolytic Degradation of a Segmented Glycolide-Trmethylene Carbonate Copolymer (Maxon<sup>®</sup>). *Polym. Degrad. Stab.*, **2007**, *92*, 975-985.
25. Li, S., Hydrolytic Degradation Characteristics of Aliphatic Polyesters Derived from Lactic and Glycolic Acids. *J. Biomed. Mater. Res.* **1999**, *48*, 342-353.
26. Raynor, J. E.; Petrie, T. A.; Garcia, A. J.; Collard, D. M., Controlling cell adhesion to titanium: Functionalization of poly(oligo(ethylene glycol)methacrylate) brushes with cell-adhesive peptides. *Adv. Mater.* **2007**, *19*, 1724-1728.

27. Gourdon, D.; Lin, Q.; Oroudjev, E.; Hansma, H.; Golan, Y.; Arad, S.; Israelachvili, J., Adhesion and stable low friction provided by a subnanometer-thick monolayer of a natural polysaccharide. *Langmuir* **2008**, *24*, 1534-1540.
28. Kobayashi, M.; Kaido, M.; Suzuki, A.; Ishihara, K.; Takahara, A., Lubrication properties of surfaces with super-hydrophilic polymer brushes. *J. Jpn. Soc. Tribol.* **2008**, *53*, 357-362.
29. Tugulu, S.; Klok, H. A., Stability and nonfouling properties of poly(poly(ethylene glycol) methacrylate) brushes-under cell culture conditions. *Biomacromolecules* **2008**, *9*, 906-912.
30. Howarter, J. A.; Youngblood, J. P., Self-cleaning and anti-fog surfaces via stimuli-responsive polymer brushes. *Adv. Mater.* **2007**, *19*, 3838-3843.
31. Kato, K.; Uchida, E.; Kang, E. T.; Uyama, Y.; Ikada, Y., Polymer Surface with Graft Chains. *Prog. Polym. Sci.* **2003**, *28*, 209-259.
32. Tam, T. K.; Ornatska, M.; Pita, M.; Minko, S.; Katz, E., Polymer brush-modified electrode with switchable and tunable redox activity for bioelectronic applications. *J. Phys. Chem. C* **2008**, *112*, 8438-8445.
33. Zhou, F.; Biesheuvel, P. M.; Chol, E. Y.; Shu, W.; Poetes, R.; Steiner, U.; Huck, W. T., Polyelectrolyte brush amplified electroactuation of microcantilevers. *Nano Lett.* **2008**, *8*, 725-730.
34. Brittain, W.; Minko, S., A Structural Definition of Polymer Brushes. *J. Polym. Sci.: Part A: Polym. Chem.* **2007**, *45*, 3505-3512.
35. Zhao, B.; Brittain, W. J., Polymer Brushes: Surface-Immobilized Macromolecules. *Prog. Polym. Sci.* **2000**, *25*, 677-710.
36. Halperin, A.; Tirrell, M.; Ledge, T. P., *Adv. Polym. Sci.* **1992**, *100*, 31.

37. Solis, F. J.; Pickett, G. T., On the Stability of the Alexander Polymer Brush. *Macromol.* **1995**, *28*, 4307-4312.
38. Van der Waarden, M., Adsorption of Aromatic Hydrocarbons in Nonaromatic Media on Carbon Black. *Colloid Sci.* **1951**, *6*, 443-449.
39. Van der Waarden, M., Stabilization of Carbon-Black dispersions in Hydrocarbons. *Colloid Sci.* **1950**, *5*, 317-326.
40. Marques, C.; Joanny, J. F., Adsorption of Block Copolymers in Selective Solvents. *Macromol.* **1988**, *21*, 1051-1059.
41. Parsonage, E.; Tirrell, M., Adsorption of Poly(2-vinylpyridine)-Poly(styrene) Block Copolymers from Toluene Solutions. *Macromol.* **1991**, *24*, 1987-1995.
42. Duda, A.; Penczek, S., Thermodynamics of L-lactide polymerization equilibrium monomer concentration. *Macromol.* **1990**, *23*, 1636-1639.
43. Edmondson, S.; Osborne, V. L.; Huck, W. T., Polymer Brushes via Surface-Initiated Polymerizations. *Chem. Soc. Rev.* **2004**, *33*, 14-22.
44. Rouse, J.; Ferguson, G. S., Stewise Formation of Ultrathin Films of a Titanium(Hydro)Oxide by Polyelectrolyte-Assisted Adsorption. *Adv. Mater.* **2002**, *14*, 151-154.
45. Efimenko, K.; Genzer, J., How to Prepare Tunable Planar Molecular Chemical Gradients. *Adv. Mater.* **2001**, *13*, 1560-1564.
46. Wu, T.; Efimenko, K.; Vlcek, P.; Subr, V.; Genzer, J., Formation and Properties of Anchored Polymers with a Gradual Variation of Grafting Densities on Flat Substrates. *Macromol.* **2003**, *36*, 2448-2453.

47. Wu, T.; Efimenko, K.; Genzer, J., Combinatorial study of the mushroom-to-brush crossover in surface anchored polyacrylamide. *J. Am. Chem. Soc.* **2002**, *124*, 9394-9395.
48. Tam, T. K.; Pita, M.; Trotsenko, O.; Motornow, M.; Tokarev, I.; Halamek, J.; Minko, S.; Katz, E., Reversible “Closing” of an Electrode Interface Functionalized with a Polymer Brush by an Electrochemical Signal. *Langmuir* **2010**, *26*, 4506-4513.
49. Motornov, M.; Tam, T. K.; Pita, M.; Tokarev, I.; Katz, E.; Minko, S., Switchable Selectivity for Gating Ion Transport with Mixed Polyelectrolyte Brushes: Approaching ‘Smart’ Drug Delivery Systems. *Nanobiotech.* **2009**, *20*, 1-11.
50. Xia, F.; Feng, L.; Wang, S.; Sun, T.; Song, W.; Jiang, W.; Jiang, L., Dual-Responsive Surfaces That Switch between Superhydrophilicity and Superhydrophobicity. *Adv. Mater.* **2006**, *18*, 432-436.
51. Santer, S.; R uhe, J., Motion of Nano-Objects on Polymer Brushes. *Polymer* **2004**, *45*, 8279-8297.
52. Spruijt, E.; Choi, E. Y.; Huck, W. T. S., Reversible Electrochemical Switching of Polyelectrolyte Brush Surface Energy Using Electroactive Counterions. *Langmuir* **2008**, *24*, 11253-11260.
53. Sun, T. L.; Wang, G. J.; Feng, L. L.; Liu, B. Q.; Ma, Y. M.; Jiang, L.; Zhu, D., Reversible Switching between Superhydrophilicity and Superhydrophobicity. *Angew. Chem. Int. Ed.* **2004**, *43*, 357-360.
54. Turgman-Cohen, S.; Genzer, J., Computer Simulation of Controlled Radical Polymerization: Effect of Chain Confinement Due to Initiator Grafting Density and Solvent Quality in “Grafting From” Method. *Macromol.* **2010**, *43*, 9567-9577.
55. Choi, I. S.; Langer, R., Surface-initiated polymerization of L-lactide: Coating of Solid Substrates with a Biodegradable Polymer. *Macromol.* **2001**, *34*, 5361-5363.

56. Tretinnikov, O. N.; Kato, K.; Iwata, H., Adsorption of Enantiomeric Poly(lactide)s on Surface-Grafted Poly(L-lactide). *Langmuir* **2004**, *20*, 6748-6753.
57. Xu, L.; Gorman, C. B., Poly(lactic acid) Brushes Grow Longer at Lower Temperatures. *J. Polym. Sci. Part A: Polym. Chem.* **2010**, *48*, 3362-3367.
58. Wang, C.; Dong, Y.; Tan, H., Biodegradable Brushlike Graft Polymers. I. Polymerization of  $\epsilon$ -Caprolactone onto Water-Soluble Hydroxypropyl Celulose as the backbone by the Protection of the Trimethylsilyl Group. *J. Poly Sci. Part A: Polym. Chem.* **2002**, *41*, 273-280.
59. Mao, J.; Gan, Z., Amphiphilic PEG-co-PGL-g-PCL Copolymer Brushes: Synthesis, Micellization and Controlled Drug Delivery. *Macromol. Chem. Phys.*, **2009**, *210*, 2078-2086.
60. Zhang, W.; Li, Y.; Liu, L.; Sun, Q.; Shuai X.; Zhu, W.; Chen, Y., Amphiphilic Toothbrushlike Copolymers Based on Poly(ethylene glycol) and Poly( $\epsilon$ -caprolactone) as Drug Carriers with enhanced Properties. *Biomacromol.* **2010**, *11*, 1331-1338.
61. Archer, R. J., Ellipsometry in the Measurement of Surface and Thin Films. Washington, DC: US. Government Printing Office; **1964**.
62. Eugene, I. *Surfaces, Interfaces, and Thin Films for Microelectronics*; John Wiley and Sons, Inc., Publication: New Jersey, 2008; pp. 257-261.

## **Chapter 2: Application of Standardized Polymer Brush Growth Conditions for Poly(lactic acid) to the Growth of Poly(glycolic acid) and Poly( $\epsilon$ -caprolactone) Brushes**

### **2.1. Introduction**

#### **2.1.1. Optimal growth conditions previously determined for poly(lactic acid) brushes**

Polymer brushes, in general, display a unique attribute compared to bulk polymer in that one end of each polymer chain is tethered to a surface. The structural orientation and flexibility of the polymer chains that result from surface confinement is perhaps the most interesting characteristic of polymer brushes.<sup>1</sup> In this chapter the growth of poly(lactic acid) (PLA), poly(glycolic acid) (PGA) and poly( $\epsilon$ -caprolactone) (PCL) brushes in homopolymer form will be discussed and the results obtained from brush growth experiments will be presented.

The most commonly used approach for lactone based polymer brush growth is through surface-initiated ring-opening polymerization (SI-ROP) of the monomer.<sup>2</sup> SI-ROP is susceptible to contamination from side products or deactivation, however.<sup>3</sup> As a result, reports on the growth of PLA brushes vary greatly in their reported ellipsometric thicknesses. Choi et al. prepared 70 nm PLA brushes using an amino silane self-assembled monolayer, SAM, on silicon as the initiator and polymerization of lactide in tetrahydrofuran, THF, at 80 °C.<sup>4</sup> Tretinnikov et al. reported 35 nm PLA brushes by using a similar hydroxyl-terminated thiol SAM on gold as the initiator and polymerization of lactide in toluene at 60 °C.<sup>5</sup> Work published by Xu suggests only 12 nm PLA brushes after using a hydroxyl-

terminated thiol SAM on gold as the initiator and polymerization of L-lactide in THF at 40 °C.<sup>6</sup> Reported thicknesses for each of these examples were obtained after 72 hours of reaction time.

The large variations in reported thicknesses are thought to be attributed to the differences in the brush preparation methods. The ability to accurately control the synthesis of SI-ROP PLA brush growth would be a promising step forward in the development of biodegradable thin films. To address this issue, a previous group member, Dr. Lebo Xu, developed a set of standard conditions that yield reproducible growth for PLA brushes. The shortest length of time required for maximum brush thickness was also determined – something that can prove beneficial for larger scale reactions. A summary of Xu’s work is provided here.

Xu investigated PLA brush growth by varying reaction temperature. Brushes were grown at four separate temperatures, 5 °C, 25 °C, 40 °C and 60 °C, over a period of 24 h. PLA brush growth at 40 and 60 °C was rapid at first reaching a maximum thickness after only a few hours (75 Å and 80 Å respectively) but ultimately decreased in thickness as time progressed. PLA brush growth at 5 °C continuously increased in thickness but grew slowly, reaching a maximum thickness of only ca. 40 Å after 24 h (Figure 1).<sup>6</sup> It was found that samples reacted at ca. 25 °C grew the best (ca. 100 Å). The term ‘best’ refers to brush growth with the greatest ellipsometric thickness in the shortest length of time. Thus, a set of standard reaction conditions for optimized PLA brush growth was successfully established through the work completed by Xu (see Experimental Details).

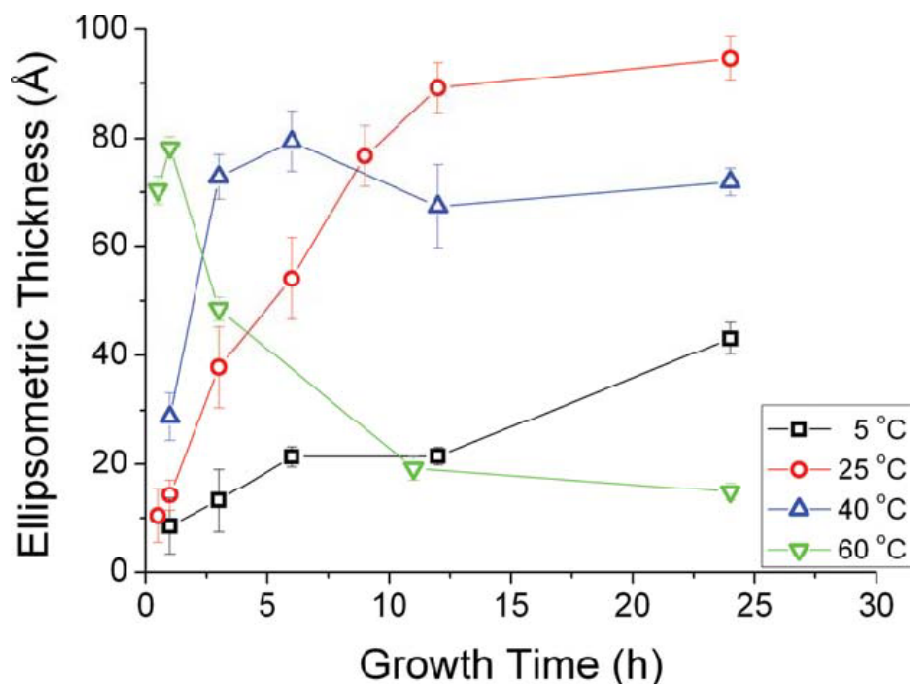


Figure 2.4: Plots of ellipsometric thicknesses vs. growth time at different temperatures. Reaction conditions: [L-lactide] = 0.1 M, [Sn(Oct)<sub>2</sub>] = 0.001 M, 24 h. Error bars represent the magnitude of the 90% confidence interval for five measurements on a single sample. This data was completed by Dr. Lebo Xu has been reproduced here for exemplary purposes.<sup>6</sup>

The reproducibility of PLA brush growth will aid researchers in the further development of temporary, thin film coatings. Additionally, there are other similar types of biocompatible polyesters that may benefit from use of the reaction conditions set forth by Xu for polymer brush growth. PGA and PCL, synthesized from glycolide and  $\epsilon$ -caprolactone respectively, are two other types of biocompatible polyesters that can also be synthesized from ROP.<sup>7,2</sup> The purpose of the work presented in the proceeding sections is to apply the optimal conditions established by Xu for PLA brush growth to the synthesis of PGA and PCL brushes.

## **2.2. Results and Discussion**

### **2.2.1. Reproducing Poly(lactic acid) brush growth**

First, prior to investigating the growth of PGA and PCL brushes, attempts were made to reproduce the PLA brush growth reported by Xu. The effort to reproduce previous findings was necessary to ensure that the same parameters were being employed in all cases. Consistency was especially important when working with the ROP synthesis method, where the yield (or molecular weight) can vary greatly with small changes in reaction conditions. The ‘standard’ parameters and reaction conditions used have been described in the Experimental Details (Section 2.3).

The first two trials exemplified the importance of using dry solvent and purified starting material (Figure 2.5). After the first trial did not produce the expected results – PLA brush growth at 25 °C similar to Figure 2.4 – it was suspected that either the solvent used (tetrahydrofuran, THF) was not dry and/or the starting monomer (L-lactide) was not of high purity. In effort to determine the quality of the THF a sodium-benzophenone test was carried out in the drybox. The results from this test confirmed that the THF used was not dry. Steps were taken to more rigorously dry the THF (see the Experimental Details). The dry solvent was used in Trial 2 for PLA brush growth.

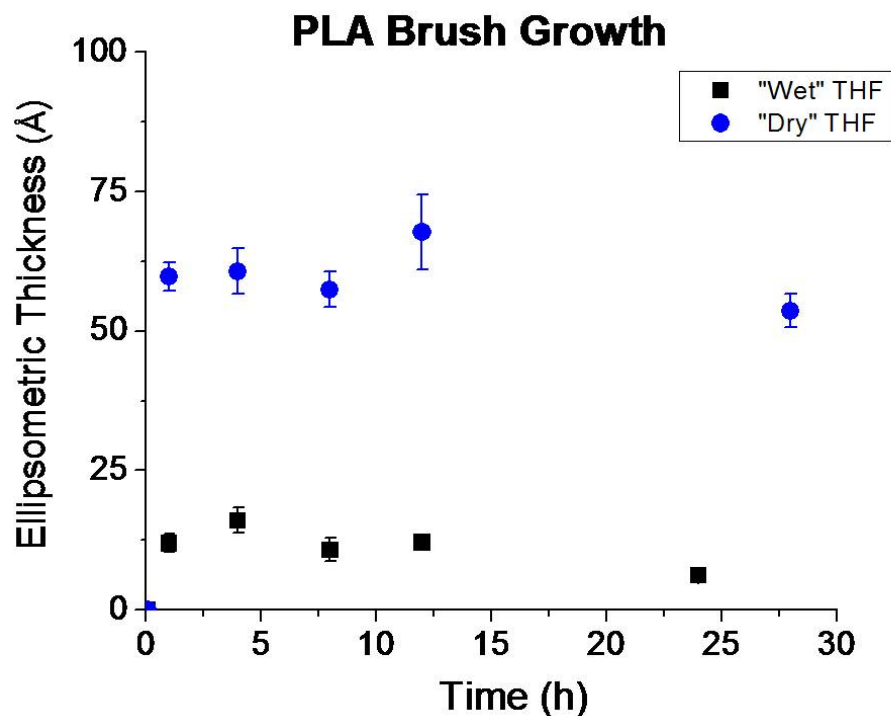


Figure 2.5: Plots of ellipsometric thicknesses of PLA brushes versus growth time. Plots represent the result of PLA brushes synthesized with water contaminated THF (black squares) and impure monomer (blue circles). Reaction conditions: [L-lactide] = 0.1 M, [Sn(Oct)<sub>2</sub>] = 0.001 M, 19 °C. Error bars represent the magnitude of the 90% confidence interval for 10 measurements across two samples.

Based on the result from Trial 2 (Figure 2.5, blue circles) attention was focused on the monomer purity and the method used for L-lactide recrystallization. The presence of water in the monomer was suspected; NMR spectra (not shown) confirmed this. Thus, Trial 3 was carried out using L-lactide that had been through four (instead of two) recrystallization cycles and was kept under reduced pressure for 48 h (as opposed to 12 h) prior to use. In addition, the PLA brushes in this trial were grown in three separate sets with overlapping reaction times (Figure 2.6).

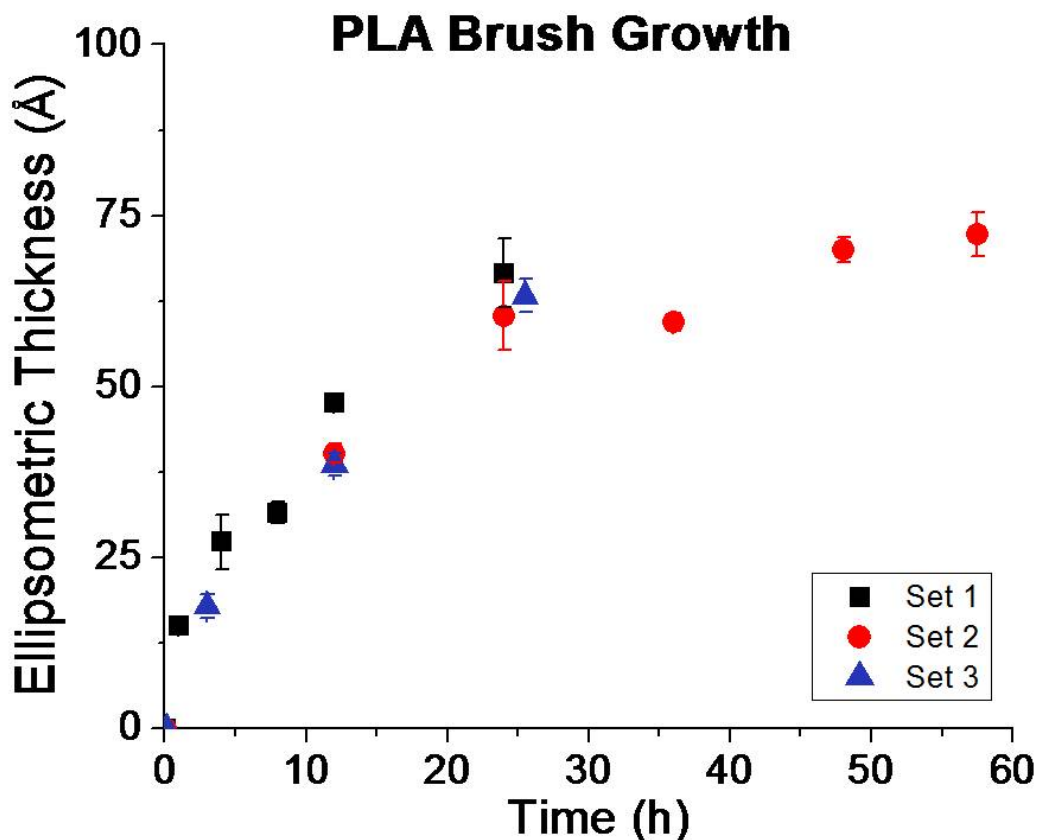


Figure 2.6: Plots of ellipsometric thicknesses of PLA brushes versus growth time. Plots represent the result of PLA brushes synthesized in dry solvent with pure monomer. Reaction conditions: high purity [L-lactide] = 0.1 M, [Sn(Oct)<sub>2</sub>] = 0.001 M, 19 °C. Error bars represent the magnitude of the 90% confidence interval for 10 measurements across two samples.

Up to this point, all PLA brush samples were synthesized under ambient temperature. As the data in Figure 2.6 still did not reproduce the growth curve reported by Xu and Gorman, it was decided to better control temperature. Moreover, as brush growth is a heterogeneous reaction, the method of agitation of the solution against the substrate was possibly a concern. To control both of these variables, Trial 4 employed the use of an

incubated rotating stage. Figure 2.7 shows thickness versus time for PLA brushes that were grown at a controlled temperature of 28 °C with slow rotation (100 RPM). The black data points are the results of this work and compare well with Xu's work (red data points).

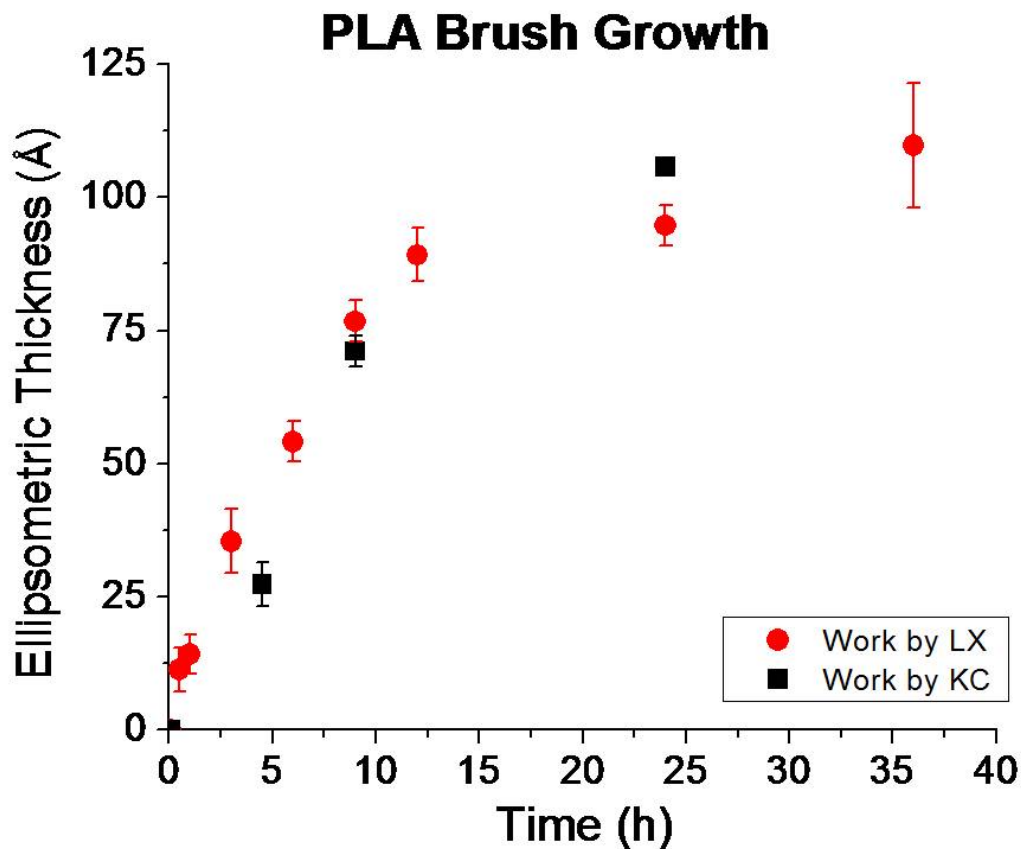


Figure 2.7: Plots of ellipsometric thicknesses of PLA brushes versus growth time. Reaction conditions: high purity [L-lactide] = 0.1 M, [Sn(Oct)<sub>2</sub>] = 0.001 M. Red circles are published data from Xu, ca. 25 °C. Black squares represent the reproducibility of Xu's work, 28 °C. Error bars represent the magnitude of the 90% confidence interval for 10 measurements across two samples.

Following the successful reproduction of Xu's work, additional characterization methods were employed to support the formation of PLA brushes on a surface. These included contact angle goniometry and attenuated total reflectance Fourier transform infrared spectroscopy (ATR-FTIR). As shown in Figure 2.8, as the ellipsometric thickness of the PLA brush samples increased the water contact angle measurements also increased. Since PLA is relatively hydrophobic compared to the original sample surface (silicon treated with hydroxyl groups), the increased contact angle with ellipsometric thickness was expected. The ATR-FTIR spectra of the sample surfaces also suggest PLA brush growth as indicated by the carbonyl stretch at  $\sim 1700\text{ cm}^{-1}$  and the C-H stretch at  $\sim 2000\text{ cm}^{-1}$  (Figure 2.9).

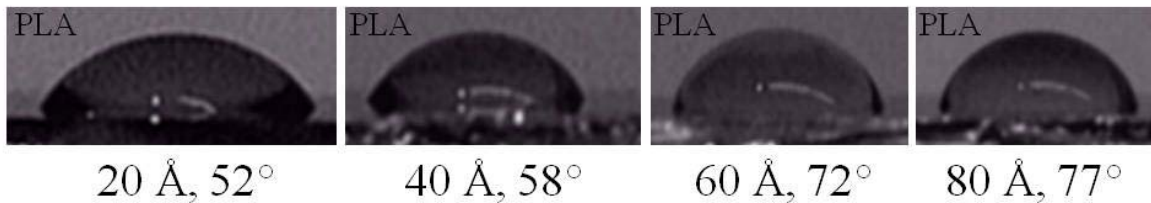


Figure 2.8: DI water contact angle measurements on PLA brush samples with increasing ellipsometric thickness.

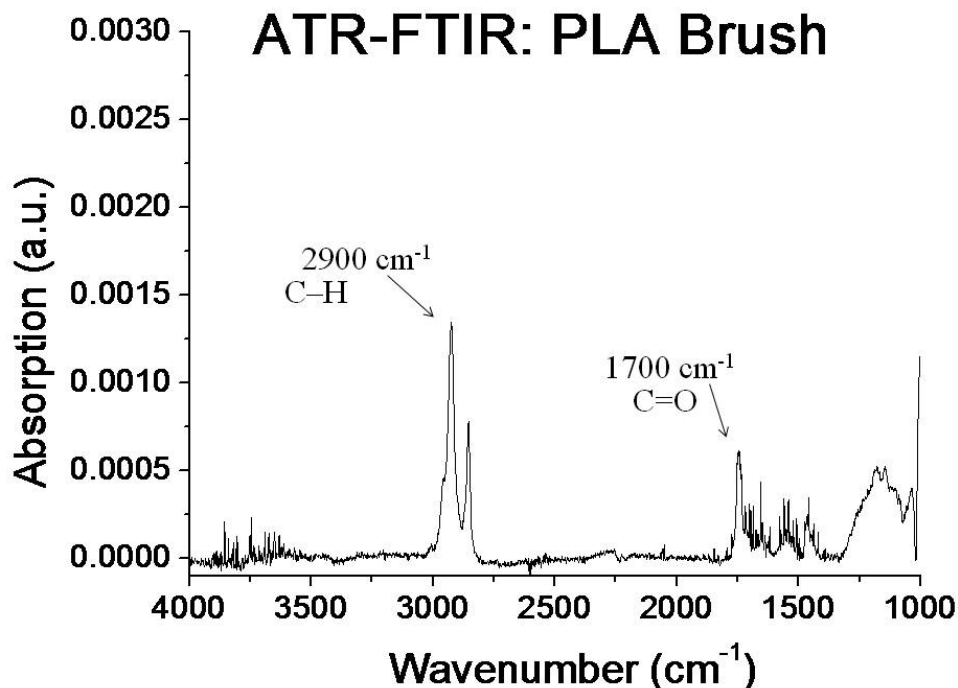


Figure 2.9: ATR-FTIR of PLA Brush sample with ca. 100 Å ellipsometric thickness.

### 2.2.2. Poly(glycolic acid) brush growth

At this point, reproducible PLA brush growth had been established. Thus, attention was focused on establishing PGA and PCL brush growth following similar suit. All reaction conditions were held constant except the monomer type, glycolide instead of L-lactide, and the recrystallizing solvent, ethyl acetate followed by acetonitrile instead of toluene. The change in recrystallization solvent was based on the lower melting point of glycolide (ca. 88 °C) compared to L-lactide (ca. 115 °C). Figure 2.10 shows the change in PGA brush growth as a function of time.

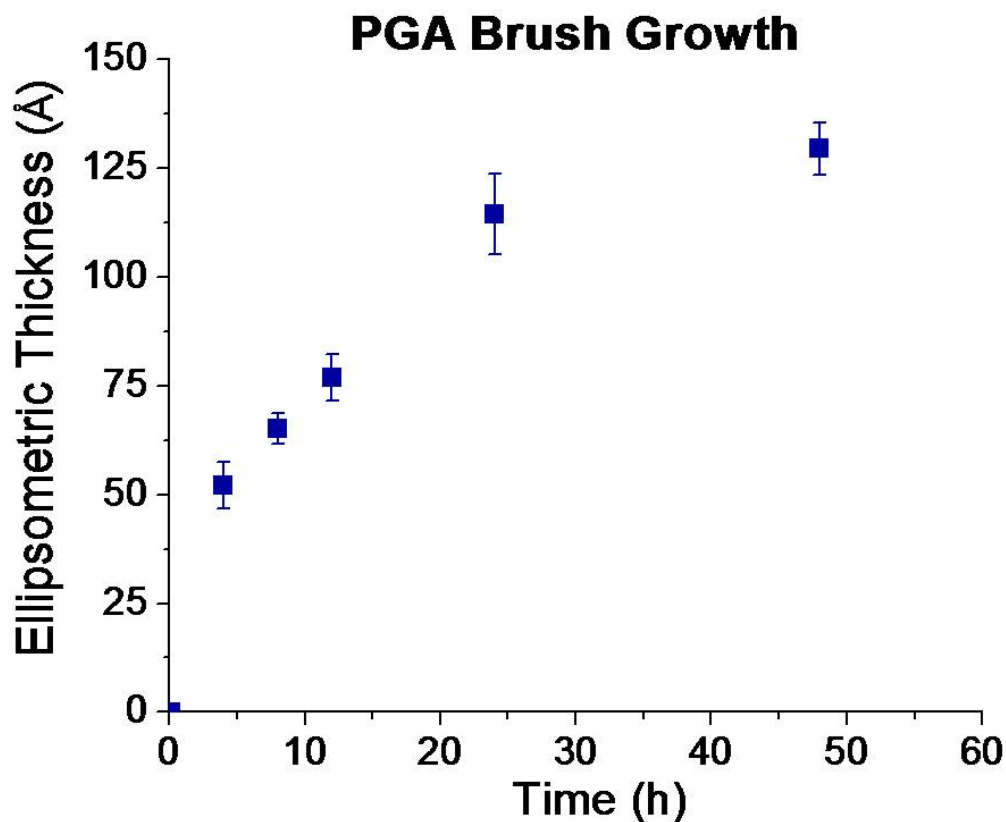


Figure 2.10: Plots of ellipsometric thicknesses of PLA brushes versus growth time. Reaction conditions: [glycolide] = 0.1 M, [Sn(Oct)<sub>2</sub>] = 0.001 M, 28 °C. Error bars represent the magnitude of the 90% confidence interval for 10 measurements across two samples.

PGA brush growth using the standard conditions was successful. The ellipsometric thickness measured after 24 h was ca. 110 Å, this is slightly greater than the maximum PLA brush thickness reported previously for the same reaction time (ca. 100 Å). Maximum PGA brush thickness was reported after a longer reaction time than PLA, however. The thickest PGA brush growth was obtained after ca. 50 h with ca. 125 Å. Otherwise, the general shape of the brush growth v. time curve for both PGA and PLA brushes were similar.

Goniometry and ATR-FTIR were also used to characterize the PGA brushes. Optical images of the water contact angles in Figure 2.11 show that the sample surface became more hydrophobic as the PGA brush thickness increased. Since PGA is relatively hydrophobic compared to the original sample surface (silicon treated with hydroxyl groups), the increased contact angle with ellipsometric thickness was expected. The ATR-FTIR spectra of Si surfaces with PGA grafted from them also suggest polymer brush growth as indicated by the carbonyl stretch at  $\sim 1700\text{ cm}^{-1}$  and the C-H stretch at  $\sim 2000\text{ cm}^{-1}$  (Figure 2.12).

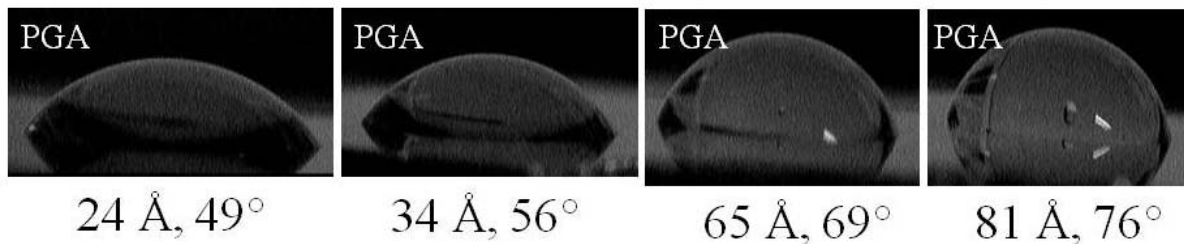


Figure 2.11: DI water contact angle measurements on PGA brush samples with increasing ellipsometric thickness.

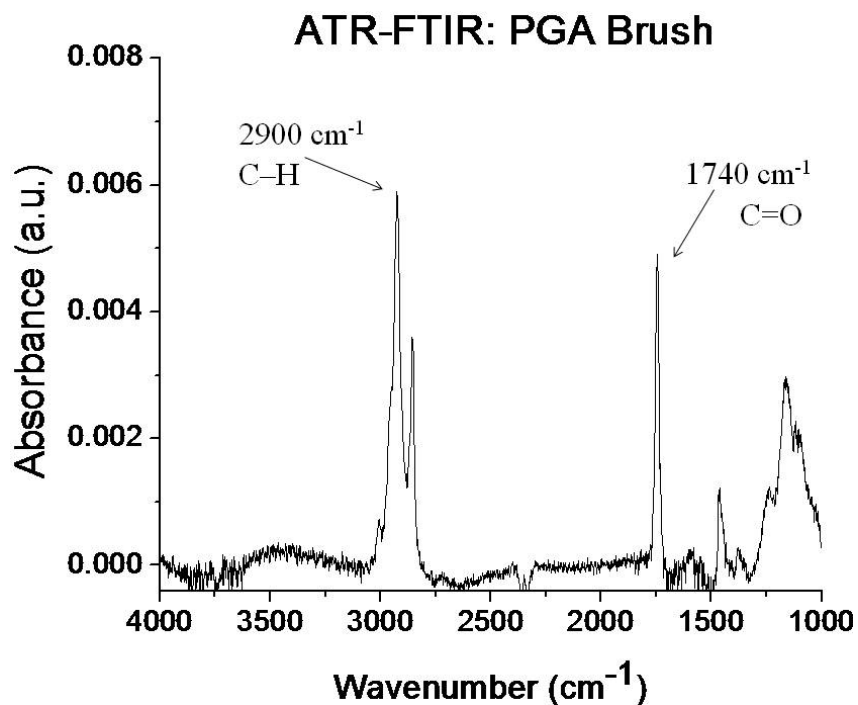


Figure 2.12: ATR-FTIR of PGA Brush sample with ca. 100 Å ellipsometric thickness.

The results from this work show that brush growth for PGA follows a similar trend when compared to the brush growth for PLA at ca. 25 °C. Though PGA brush-like reports have been made in literature,<sup>8</sup> this is the first report of a PGA homopolymer brush growth curve. This is a promising step forward towards the development of biodegradable thin film coatings. It would be interesting to investigate PGA growth trends under different reaction conditions to see if any further increase in brush thickness occurs – this will be the primary focus of Chapter 3.

### 2.2.3. Poly( $\epsilon$ -caprolactone) brush growth

As discussed in Chapter 1, PCL brushes have been prepared previously.<sup>9,10</sup> However, similar to the different PLA brush thicknesses reported in literature,<sup>4,5</sup> reports on PCL brush thicknesses also vary a great deal.<sup>11,12,13</sup> Thus, in an effort to establish a set of standard procedures for the SI-ROP of PCL, brushes were synthesized using the same standard conditions that had been employed for PLA and PGA brushes (Figure 2.13).

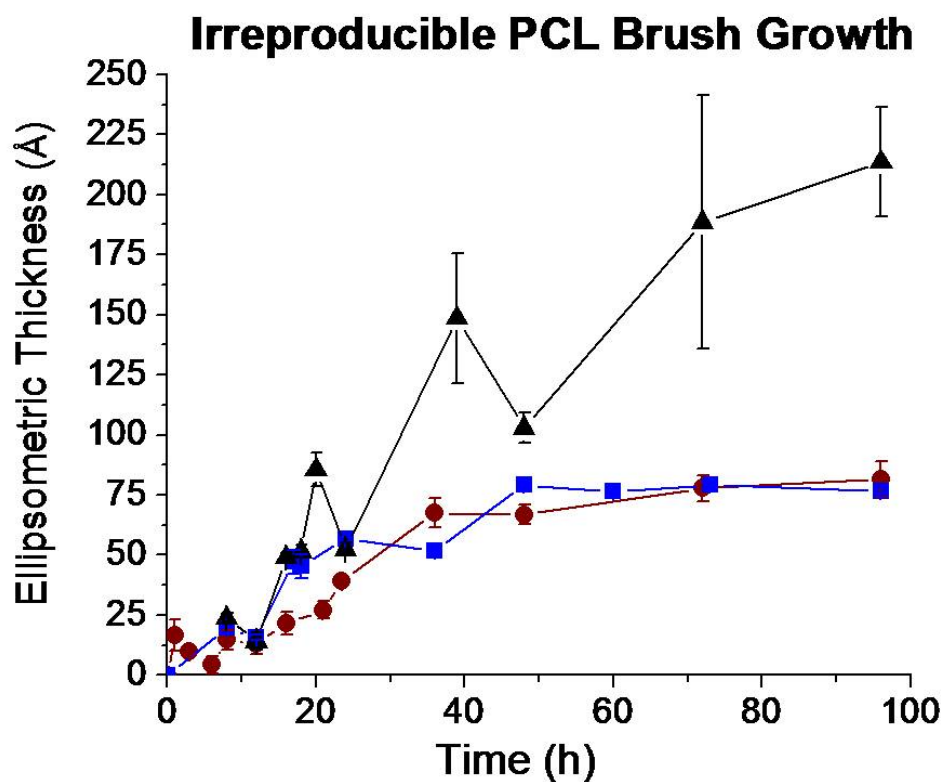


Figure 2.13: Plots of ellipsometric thicknesses of PLA brushes versus growth time. Plots show the irreproducibility of PCL brushes under the same reaction conditions: [ $\epsilon$ -caprolactone] = 0.1 M, [ $\text{Sn}(\text{Oct})_2$ ] = 0.001 M, ca. 25 °C. Error bars represent the magnitude of the 90% confidence interval for 10 measurements across two samples.

Though promising, the attempts to reproducibly grow PCL brushes were not successful. The three separate trials carried out for PCL brush growth did not show similar growth kinetics despite using the same reaction conditions. Nevertheless, additional characterization was carried out to confirm that PCL brush growth had occurred. Optical images of deionized water contact angles were taken on four separate samples, each with increasing thickness (Figure 2.14). The images show that the sample surface became more hydrophobic as the PCL brush thickness increased. Since PCL is relatively hydrophobic compared to the original sample surface (silicon treated with hydroxyl groups), the increased contact angle with increasing ellipsometric thickness was expected. The ATR-FTIR spectra of Si surfaces with PCL grafted from them also suggest polymer brush growth as indicated by the carbonyl stretch at  $\sim 1700\text{ cm}^{-1}$  and the C-H stretch at  $\sim 2000\text{ cm}^{-1}$ .

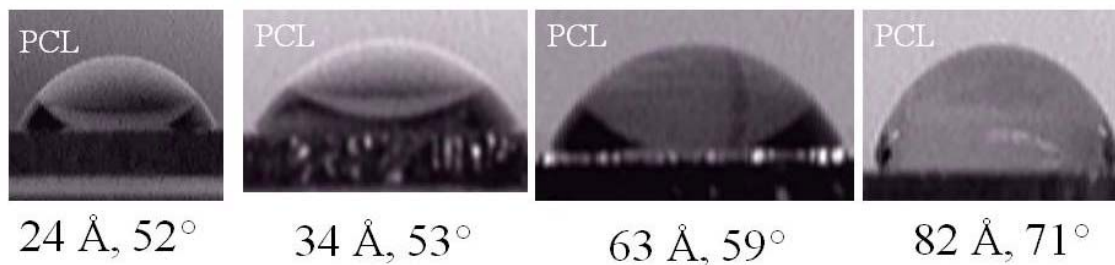


Figure 2.14: DI water contact angle measurements on PCL brush samples with increasing ellipsometric thickness.

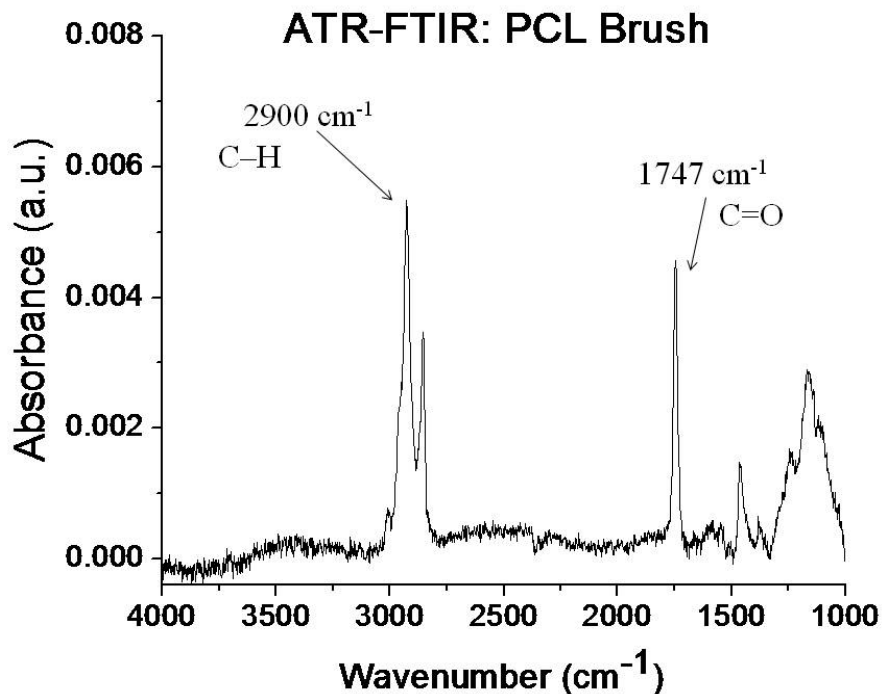


Figure 2.15: ATR-FTIR of PCL Brush sample with ca. 100 Å ellipsometric thickness.

The irreproducibility of PCL brush thickness under these conditions is thought to be attributed to a combination of the presence of water in the reaction system and the lower reactivity of the monomer. The driving force behind the ROP of lactones is the release of ring strain.<sup>2</sup> Since  $\epsilon$ -caprolactone has less ring strain than both L-lactide and glycolide, it is inherently less reactive towards ROP. Hence, continued development of the synthesis method for PCL brushes is required. It is anticipated that with a monomer of high purity, and under the right reaction conditions, reproducible PCL brush growth can be established. Thus, further investigation of PCL brush growth is better fit as a separate project and will no longer be included in the scope of this thesis.

## **2.3. Conclusion**

The standard reaction conditions developed by Xu for PLA brush growth were applied to PGA and PCL brushes in effort to establish similar growth kinetics (or behaviors). It was found that under the same reaction conditions, PGA brush growth was similar to that of PLA brushes. The growth of PCL brushes, however, did not follow the same trend as PLA or PGA brushes. Although the three different polymer brush types, PLA, PGA and PCL did show an increase in brush thickness as a function of time, the brush trends for PCL were not reproducible. However, the success of PGA brush growth when using the standard conditions has provided a promising step forward in the advancement of biodegradable thin film coatings.

## **2.4. Experimental Details**

### **2.4.1. Si chip preparation**

Silicon substrates were cut in to 1.5 cm × 2.0 cm pieces from 4.0” silicon wafers with [100] orientation (Wafer World, Inc.). Once dried the Si samples were placed in an ultra-violet ozonolysis, UVO instrument for 40 minutes unless noted otherwise. Cleaned Si chips were measured via ellipsometry (for initial thickness) and then taken to the dry box for polymer brush sample preparation.

### **2.4.2. Polymer brush growth preparation**

The oxide layer on freshly prepared Si samples was measured via ellipsometry to provide an initial surface thickness. The measured samples were then placed in clean, oven dried 20 mL vials and then taken to the drybox. Tin(II) ethyl-hexanoate ( $\text{Sn}(\text{Oct})_2$ ) was used as a catalyst for polymer brush growth. The final catalyst concentration was 0.001 M unless noted otherwise. Monomer (L-lactide, glycolide or  $\epsilon$ -caprolactone) was slowly added to each sample vial (5 mL of 0.1 M in THF). Sample vials were sealed tightly with Teflon caps. Prepared samples were then taken to an incubated environment to ensure constant temperature (28 °C) and rotation speed (100 RPM) unless otherwise noted.

### **2.4.3. Reaction quenching**

After the specified reaction time had been reached, samples were removed from the reaction environment, placed in 5 mL anhydrous tetrahydrofuran, THF, and sonicated for 15 s. Following sonication, polymer brush samples were rinsed with an excess of DI water and ethanol then dried under a stream of gaseous nitrogen. Dried samples were measured via ellipsometry for a final polymer brush thicknesses. Samples were stored in sterile Petri dishes under ambient conditions.

#### 2.4.4. Distilled or recrystallized monomers and solvents

$\epsilon$ -Caprolactone, glycolide and L-lactide (Sigma Aldrich) were purified before use.  $\epsilon$ -Caprolactone was dried under  $\text{CaH}_2$  overnight then distilled under reduced pressure (ca. 120 °C and 40 mmHg). Glycolide (mp. 86-88 °C) was recrystallized twice. Once with anhydrous ethyl acetate (bp. 77.1 °C) followed by anhydrous acetonitrile (bp. 82 °C). Crystals were dried via vacuum filtration under a stream of gaseous nitrogen. Semi-dry crystals were further dried under reduced pressure (ca. 5 mTorr) for 48 h at 35 °C. L-lactide (mp. 115 °C) was recrystallized twice using anhydrous toluene (bp. 110 °C). Crystals were dried via vacuum filtration under a stream of gaseous nitrogen. Semi-dry crystals were further dried under reduced pressure (ca. 5 mTorr) for 48 h at 40 °C.

THF and toluene were distilled from sodium, benzophenone. The solvents were collected in an oven dried (nitrogen cooled) side-arm receiver flask. Ethyl acetate and acetonitrile were distilled at their respective boiling points.

All monomers and solvents were stored in a nitrogen atmosphere (dry box) sealed with Teflon fitted caps. THF and toluene were tested for dryness in the drybox after collection. The tests were carried out by adding 10  $\mu\text{L}$  of a previously prepared mixture of sodium and benzophenone to 10 mL of solvent.

## **2.4.5. Instrumentation methods**

### **2.4.5.1. Ellipsometry**

Sample thicknesses were measured by a single-wavelength ellipsometer at a 70° angle (AutoEL-III, Rudolph Research, Flanders, USA). All measurements were taken on dry samples. Five measurements, four at the corners and one at the center, were taken on each sample. Measurements were taken before and after brush growth in order to obtain a more accurate ellipsometric thickness.

### **2.4.5.2. ATR-FTIR**

The ATR-FTIR was conducted on the Excalibus Series bench (VARIAN) with the MIRacle Single Reflection ATR kits (PIKE). The ATR crystal was the Germanium crystal. The pressure to hold each sample was 530 lbs.

### **2.4.5.3. DI water contact angle**

The DI water contact angle test was measured on home-made setup. The DI water droplet image was collected by video camera (Panasonic GP-KR222). Then the image was analyzed by ImageJ software (Image J 1.32j, Wayne Rasband, National Institutes of Health, USA) to read the contact angle value.

#### 2.4.6. Glassware

20 mL reaction vials (with Teflon lids) were used throughout the polymer brush experiments. For cleaning, the vials were soaked in toluene, followed by base bath solution (isopropyl alcohol and KOH). After thorough scrubbing, the vials were rinsed with DI water and acetone respectively. Vials were purged with nitrogen gas. All glassware was used hot from overnight drying ca. 130 °C.

#### 2.5. References

1. Zhao, B.; Brittain, W. J., Polymer Brushes: Surface-Immobilized Macromolecules. *Prog. Polym. Sci.* **2000**, *25*, 677-710.
2. Edmondson, S.; Osborne, V.; Huck, W. T. S., Polymer Brushes via Surface-Initiated Polymerizations. *Chem. Soc. Rev.* **2004**, *33*, 14-22.
3. Brittain, W. J.; Mink, S., A Structural Definition of Polymer Brushes. *J. Polym. Sci. Part A: Chem.* **2007**, *45*, 3505-3512.
4. Choi, I. S.; Langer, R., Surface-initiated polymerization of L-lactide: Coating of Solid Substrates with a Biodegradable Polymer. *Macromol.* **2001**, *34*, 5361-5363.
5. Tretinnikov, O. N.; Kato, K.; Iwata, H., Adsorption of Enantiomeric Poly(lactide)s on Surface-Grafted Poly(L-lactide). *Langmuir* **2004**, *20*, 6748-6753.
6. Xu, L.; Gorman, C. B., Poly(lactic acid) Brushes Grow Longer at Lower Temperatures. *J. Polym. Sci. Part A: Polym. Chem.* **2010**, *48*, 3362-3367.

7. Flieger, M.; Kantorova, M.; Prell, A.; Rezanka, T.; Votruba, J., Biodegradable Plastics from Renewable Sources. *Folia Microbiol.* **2003**, *1*, 27-44.
8. Mao, J.; Gan, Z., Amphiphilic PEG-co-PGL-g-PCL Copolymer Brushes: Synthesis, Micellization and Controlled Drug Delivery. *Macromol. Chem. Phys.* **2009**, *210*, 2078-2086.
9. Lee, H. J.; Ramaraj, B.; Yoon, K. R., Esterification on Solid Support by Surface-Initiated Ring-Opening Polymerization of  $\epsilon$ -Caprolactone from Benzylic Hydroxyl-Functionalized Wang Resin Bead. *J. Appl. Polym. Sci.* **2009**, *111*, 839-844.
10. Moon, J. H.; Ramarah, B.; Lee, S. M.; Yoon, K. R., Direct Grafting of  $\epsilon$ -caprolactone on Solid Core/Mesoporous Shell Silic Spheres by Surface-Initiated Ring-Opening Polymerization. *J. Appl. Polym. Sci.* **2008**, *107*, 2689-2694.
11. Olivier, A.; Raquez, J. M.; Dubois, P.; Damman, P., Semi-Crystalline Poly( $\epsilon$ -caprolactone) Brushes on Gold Substrate via "Grafting From" Method: New Insights with AFM Characterization. *Europ. Polym. J.* **2011**, *47*, 31-39.
12. Voccia, S.; Bech, L.; Gilver, B.; Jérôme, R.; Jérôme, C., Preparation of Poly( $\epsilon$ -caprolactone) Brushes at the Surface of Conducting Substrates. *Langmuir* **2004**, *20*, 10670-10678.
13. Husemann, M.; Mecerreyes, D.; Hawker, C. J.; Hedrick, J. L.; Shah, R.; Abbott, N. L., Surface-Initiated Polymerization for Amplification of Self-Assembled Monolayers Patterned by Microcontact Printing. *Angew. Chem.* **1999**, *111*, 688-691.

## **Chapter 3: Adjustments to Standardized Polymer Brush Growth Conditions to maximize the thickness of Poly(glycolic acid) Brushes**

### **3.1. Introduction**

#### **3.1.1. Changes to standard conditions**

The primary focus of this chapter is to determine how poly(glycolic acid) (PGA) brush growth may be affected by changes made to the sample preparation process or reaction environment. In the previous chapter, attention was focused on PGA brush growth using the standard conditions set forth by the optimal reaction parameters found for poly(lactic acid), PLA, brushes (see Chapter 2 Experimental Details). Although PGA brush growth does occur under these conditions, there may be additional adjustments that can be made to further optimize brush growth.

A previous report on the effect of temperature has been made for PLA brushes suggesting that growth is favored at ambient as opposed to elevated temperatures.<sup>1</sup> Similar conditions of increased and decreased temperature were applied here to see how temperature changes would affect PGA brush growth. In addition to the investigation of the effects of temperature, adjustments made to the Si substrate cleaning method and the technique used to prepare the brush samples were also studied. For polymer brush growth, the latter two procedures have not been clearly reported previously. However, this type of investigation is important as it would expose how variations in reaction conditions effect PGA brush growth.

### 3.3. Results and Discussion

#### 3.3.1. Effects of temperature

PGA brush growth at temperatures both above and below ambient were investigated. The previously established ‘standard’ methods (see Experimental Details) were applied to all samples. Figure 3.16 provides plots of ellipsometric thickness vs. time for PGA brush growth at four different temperatures, 8 °C, 28 °C, 37 °C and 60 °C. The results show that PGA brush growth was slowest at 8 °C with an ellipsometric thickness reaching only ca. 40 Å after 20 h. In contrast, the largest brush thickness was obtained at 28 °C with a maximum ellipsometric thickness of ca. 110 Å after 24 h. Brush growth at elevated temperatures reached a maximum ellipsometric thicknesses of ca. 80 Å after 2.5 h of reaction time for 60 °C and ca. 80 Å after 5 h for 37 °C.

The smaller ellipsometric thicknesses reported at elevated temperatures (when compared to ambient temperature) is attributed to the increased amount of bulk polymerization that occurs in solution under these conditions. The large amount of polymer precipitate from solution deposits on the sample surface. The polymer precipitant can then become physisorbed on the surface inhibiting further polymer brush growth from occurring.

Optical images of bulk polymer in solution were taken after 24 h of reaction time at 28 °C and 60 °C (Figure 3.16). The images have been included as a visual comparison so that the difference in appearance between the resulting sample vials at different temperatures can be seen. The reaction conducted at 60 °C exhibited a mostly clear bulk solution with polymer precipitate near the base of the reaction vial. In contrast, the reaction conducted at 28 °C displayed a slight cloudiness throughout the bulk solution with no polymer precipitate. The suspended cloudiness was polymer as confirmed by collection of polymer via centrifuge.

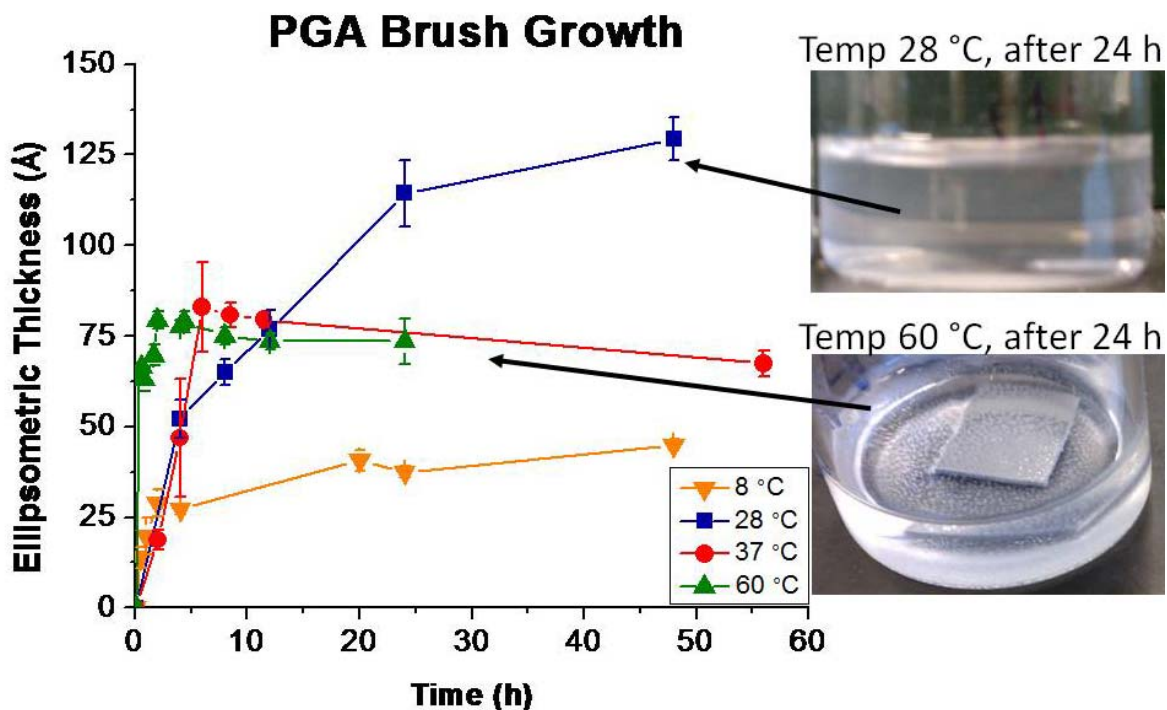


Figure 3.16: (Left) Plots of ellipsometric thickness vs. growth time for PGA brushes at 8, 28, 37 and 60 °C. Reaction conditions: [glycolide] = 0.1 M, [Sn(Oct)<sub>2</sub>] = 0.001 M, sample rotation speed = 100 RPM. Error bars represent the magnitude of the 90% confidence interval for 10 measurements across two samples. (Right) Optical images of reaction vessels after 24 h of reaction time at ambient (above) and elevated (below) temperatures.

### 3.3.2. Effects of static vs. non-static growth environments

Under standard conditions, all PGA brush samples were grown in solutions that were rotated at 100 RPM. However, to maximize PGA brush thickness the degree to which stirring may be beneficial was investigated including whether or not this type of perturbation is necessary at all. To study this effect, two alternate reaction conditions, growth without rotation and increased rotation speed (300 RPM), were applied separately to PGA brush experiments. All remaining reaction conditions were held constant throughout the

experiments. The results were compared to the PGA brush growth obtained from a rotation speed of 100 RPM (Figure 3.17).

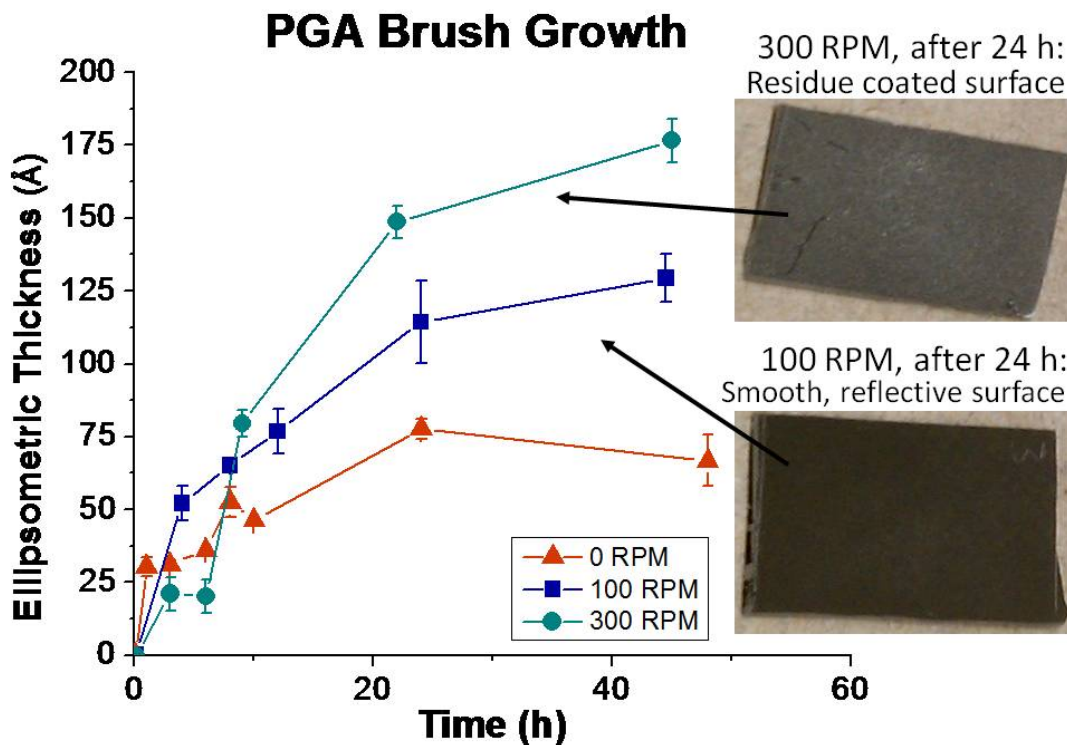


Figure 3.17: Plots of ellipsometric thickness vs. growth time for PGA brushes at 0, 100 and 300 RPM rotation speeds. Reaction conditions: [glycolide] = 0.1 M, [Sn(Oct)<sub>2</sub>] = 0.001 M, 28 °C. Error bars represent the magnitude of the 90% confidence interval for 10 measurements across two samples.

As shown in Figure 3.17, PGA brush growth from the static growth environment resulted in a maximum ellipsometric thickness of ca. 75 Å after 24 h of reaction time. This value is significantly less than the brush samples exposed to 100 RPM rotation (ca. 110 Å)

over the same 24 h period. This may have been attributed to the depletion of monomer concentration near the sample surface due to the formation of a gradient as a result of polymerization that occurred in solution.<sup>2</sup> The values for PGA brush growth at 300 RPM rotation after 24 h produced the largest ellipsometric thickness of ca. 148 Å. However, the increased stirring speed promoted polymer growth in solution resulting in physisorption of bulk PGA on the sample surface; similar to what was seen for samples grown at elevated temperatures. Thus, it was found that the high degree of mechanical mixing was too disruptive for reliable brush growth and that the reported increase in ellipsometric thickness is largely due to physisorption. Figure 3.17 provides optical images of brush samples taken after 24 h of reaction time for 100 RPM and 300 RPM. The images have been provided as a visual representation of the polymeric residue found on the sample surface after being exposed to an increase in rotation speed.

### **3.3.3. Experimental techniques**

The methods employed during the sample preparation process will likely play an important role for optimizing reproducible surface-initiated ring-opening polymerization (SI-ROP) of PGA brushes. Thus, various Si wafer cleaning methods and sample preparation techniques were investigated. A control group was used for each variation in the sample preparation method. The control was synthesized by using the previously established ‘standard’ brush growth procedure (see Experimental Details). These same procedures were

used throughout each of the experiments with the exception of changes made to the specified variables of interest.

### **3.3.3.1. Silicon sample cleaning methods**

Under standard conditions, the Si substrates used for brush growth were cleaned and then exposed to an ultra-violet light source (UVO) to form an oxide layer on the Si surface. In effort to identify the extent to which cleaning is required, five separate cleaning methods (four variations plus the control) were employed (Figure **3.18**). The variations included surface etching before UVO exposure (Method 1), sonication before UVO exposure (Method 2), the control (Method 3, 40 min UVO), less UVO exposure (Method 4, 25 min) and the least amount of UVO exposure (Method 5, 10 min).

The lowest brush thicknesses were obtained from Si samples that were exposed to cleaning treatments of etching (Method 1) and sonication (Method 2) with corresponding ellipsometric thicknesses of ca. 64 Å and 72 Å respectively. A maximum PGA brush ellipsometric thickness of ca. 85 Å was obtained from the control (Method 3). The next largest ellipsometric thicknesses were ca. 80 Å obtained from 25 min of UVO treatment (Method 4), followed by only 10 min of UVO treatment with ca. 74 Å (Method 5).

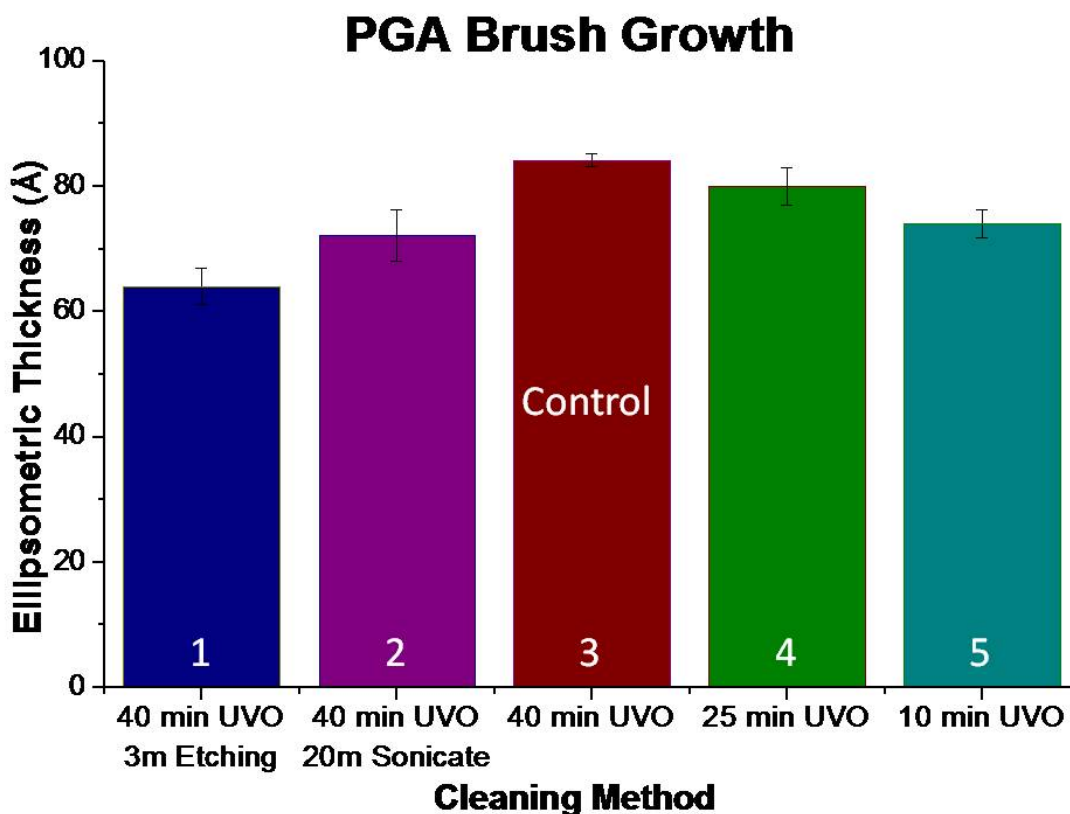


Figure 3.18: Histogram of ellipsometric thickness vs. growth time for PGA brushes after 24 h of reaction time. Reaction conditions: [glycolide] = 0.1 M, [Sn(Oct)<sub>2</sub>] = 0.001 M, sample rotation speed = 100 RPM, 28 °C. Error bars represent the magnitude of the 90% confidence interval for 10 measurements across two samples.

It was determined that exposing Si samples to sonication or etching prior to UVO treatment resulted in PGA brushes with smaller thicknesses. When exposing Si samples to UVO, the longer light irradiation times the thicker the PGA brush. However, it should be noted that, while not investigated in this work, prolonged exposure to UVO treatment can lead to deformation of the Si surface.<sup>3</sup>

### **3.3.3.2. Polymer brush preparation techniques**

Following the investigation of different Si wafer cleaning methods, several different sample preparation techniques were investigated to determine how the variation in experimental technique affected PGA brush growth. Here, the experimental conditions were adjusted by using a constant monomer volume (5 mL glycolide, 0.1 M) while varying the addition of catalyst ( $\text{Sn}(\text{Oct})_2$ ) (Figure 3.19).

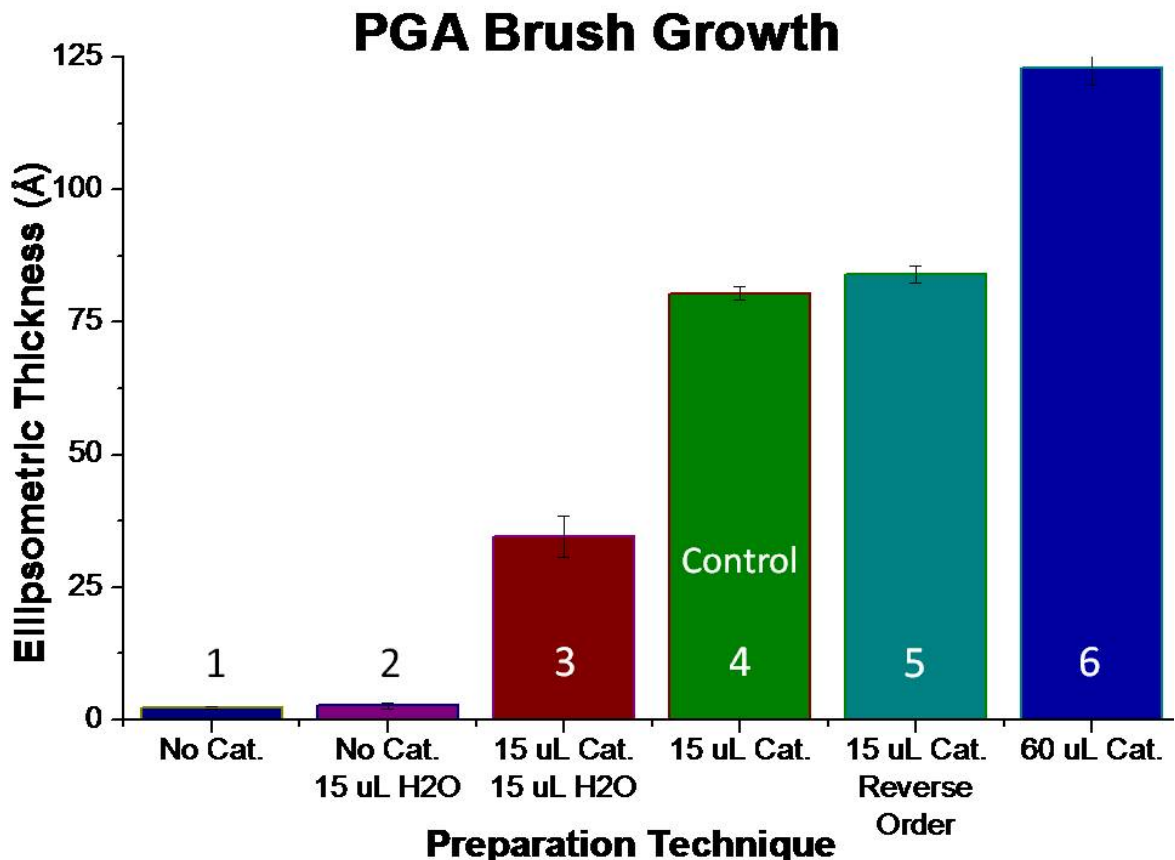


Figure 3.19: Histogram of ellipsometric thickness vs. growth time for PGA brushes after 24 h of reaction time. Data points represent six separate sample preparation methods: (1) No catalyst, (2) No catalyst but addition of H<sub>2</sub>O on sample surface, (3) 15  $\mu$ L catalyst (0.001 M) on sample surface followed by 15  $\mu$ L H<sub>2</sub>O after addition of monomer, (4) “Control” sample, 15  $\mu$ L catalyst (0.001 M) on sample surface, (5) 15  $\mu$ L catalyst (0.001 M) added after monomer and (6) 60  $\mu$ L catalyst (0.006 M) on sample surface. Remaining reaction conditions: [glycolide] = 0.1 M (5 mL aliquot for each sample), sample rotation speed = 100 RPM, 28 °C. Error bars represent the magnitude of the 90% confidence interval for 10 measurements across two samples.

Conditions 1 and 2 did not contain any catalyst and did not show any PGA brush growth. The lack of brush growth under these conditions accentuate the importance of the presence of catalyst (Sn(Oct)<sub>2</sub>) for the SI-ROP of glycolide. Condition 3 which contained catalyst and deionized H<sub>2</sub>O resulted in the least amount of brush growth with an ellipsometric

thickness of only ca. 35 Å. Minimal surface growth was obtained upon the addition of water. Water is a known initiator for bulk polymerization and may have thus resulted in a smaller concentration of monomer available for brush growth.<sup>4</sup> Conditions 4 and 5 (with number 4 being the control) have the same ellipsometric thickness (ca. 80 Å) indicating that the order of catalyst vs. monomer addition has little affect on PGA brush growth. Condition 6 had the largest ellipsometric thickness with a measurement of ca. 122 Å. However, at the end of the 24 h reaction period these samples contained visible residue on the Si surface indicating physisorption of bulk PGA polymer from solution. The residue was not easily removed with sonication. Thus, the amount of brush growth formed from technique 6 via the ‘grafting from’ method cannot be precisely determined. Instead, the reported ellipsometric thickness of ca. 122 Å was taken to be the maximum possible value with the actual brush thickness likely being a somewhat lesser value.

Next, PGA brushes were grown using different volumes of monomer. Samples were prepared using 1 mL, 3 mL, 5 mL (the control), 7 mL or 10 mL of 0.1 M glycolide (Figure 3.20). Ellipsometric measurements obtained for these samples suggest that a range of 3 – 10 mL of monomer stock solution produce similar PGA brush thicknesses (ca. 60 Å) after 24 h of reaction time. The larger ellipsometric thicknesses (ca. 375 Å) reported for the 1 mL samples can be attributed to the physisorption of bulk polymer on the surface. The large amount of polymeric residue most likely occurred because the meniscus from the stock solution was too close to the sample surface causing any formation of bulk polymer to deposit directly onto the Si substrate.

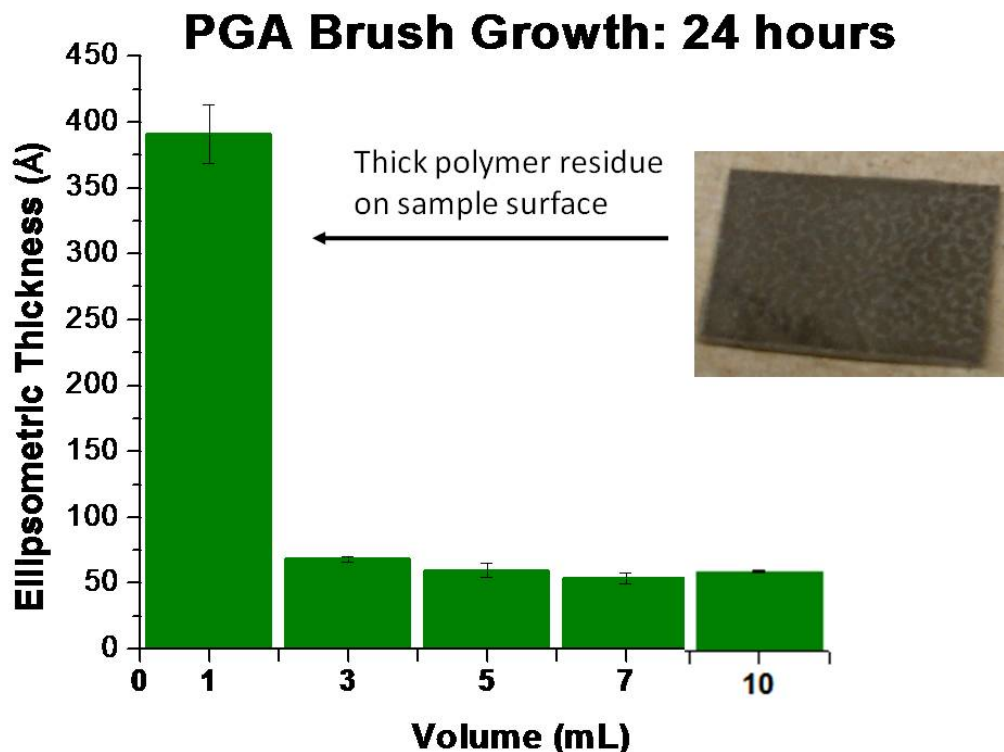


Figure 3.20: Histogram of ellipsometric thickness vs. growth time for PGA brushes after 24 h of reaction time. Reaction conditions: [glycolide] = 0.1 M, [Sn(Oct)<sub>2</sub>] = 0.001 M, sample rotation speed = 100 RPM, 28 °C. Error bars represent the magnitude of the 90% confidence interval for 10 measurements across two samples.

#### 3.3.4. Glycolide purification

All PGA brush growth experiments described in this text were synthesized using recrystallized monomer (glycolide, melting point (mp.) = 88 °C). The purpose of recrystallization was to reduce the amount of water present in the monomer. As previously mentioned, water can act as an initiator for polymerization in solution.<sup>4</sup> Work presented in the previous sections has shown that too much polymerization in solution can hinder polymerization on the surface. Additionally, it has been reported that the type of

recrystallization solvent used can affect the crystallinity of the material.<sup>5</sup> Ultimately, it is thought that a good choice of solvent could lead to an increase in monomer purity. In effort to determine the effect of the recrystallization solvent on PGA brush growth four trials of monomer recrystallization were completed, each with a different solvent combination (Figure 3.21).

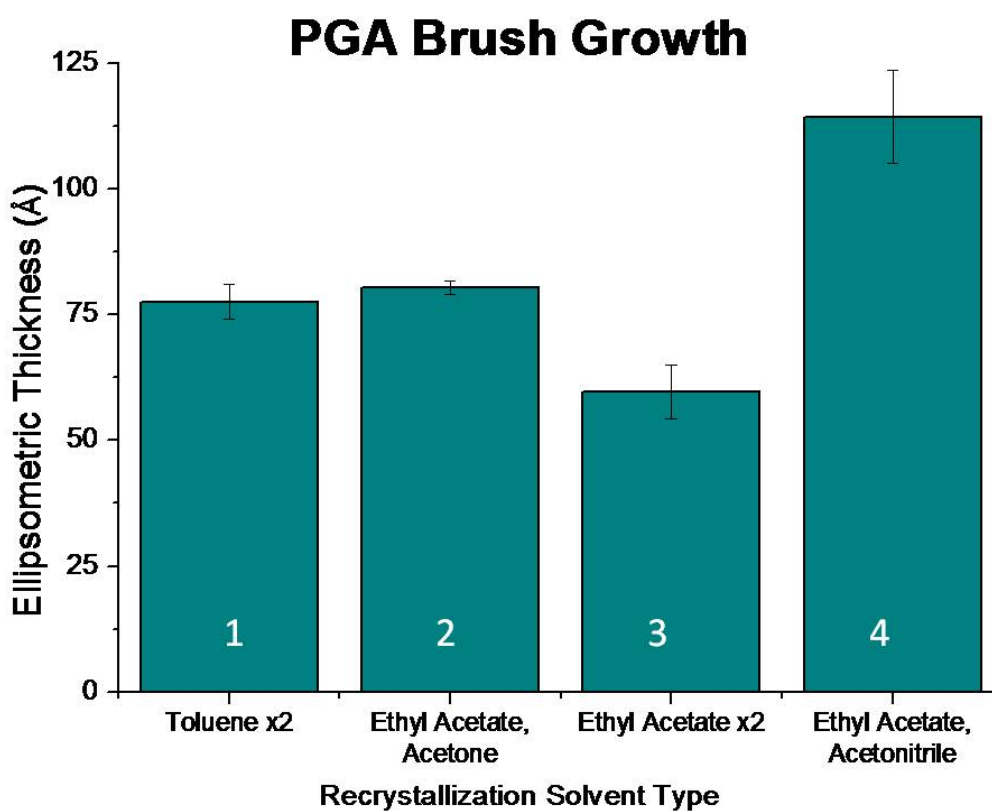


Figure 3.21: Histogram of ellipsometric thickness vs. growth time for PGA brushes after 24 hours of reaction time for brushes grown using glycolide recrystallized from different solvents. Trial 1: toluene only (twice recrystallized); trial 2: ethyl acetate followed by acetone; trail 3: ethyl acetate only (twice recrystallized); trial 4: ethyl acetate followed by acetonitrile. All solvents were anhydrous. Reaction conditions: [glycolide] = 0.1 M, [Sn(Oct)<sub>2</sub>] = 0.001 M, sample rotation speed = 100 RPM, 28 °C. Error bars represent the magnitude of the 90% confidence interval for 10 measurements across two samples.

When toluene was used as a recrystallization solvent (Trial 1, boiling point (bp.) = 110 °C) ellipsometric thicknesses of ca. 77 Å were obtained after 24 h of reaction time. The use of ethyl acetate followed by acetone for recrystallization (Trial 2, bp. = 77 °C and 56 °C respectively) produced PGA brushes of ca. 80 Å thickness. Ethyl acetate as a recrystallization solvent (Trial 3) produced ellipsometric thicknesses of only ca. 60 Å after 24 h of reaction time. However, when ethyl acetate was followed by acetonitrile for recrystallization (Trial 4, bp. = 82 °C for acetonitrile) ellipsometric thicknesses of ca. 110 Å were obtained.

The variation of ellipsometric thickness across different solvent types/combinations may be attributed to the difference in the boiling point of the solvent(s) vs. the melting point of the monomer. Generally, when selecting a recrystallization solvent the boiling point should be below, but as close to, the melting point of the monomer as possible. If the monomer is allowed to melt before the solvent boils, then the material precipitates without well defined crystals.<sup>5</sup> Thus, the recrystallizations carried out using toluene (bp. = 110 °C) produced a paste-like glycolide precipitate (glycolide mp. = 88 °C). In contrast, glycolide recrystallized with acetonitrile (bp. = 82 °C) produced the thickest brushes; this was likely attributed to the minimal difference between the monomer melting point and the solvent boiling point.

### **3.4. Conclusion**

PGA brush growth reproducibility is paramount if it is to be considered for larger scale applications. Thus, the reaction parameters required for optimal PGA brush growth (measured via ellipsometric thickness) in the shortest length of time need to be determined. In this light, several parameters were investigated in effort to develop the most efficient/dependable PGA brush growth method.

PGA brushes grew best at room temperature after 24 h of reaction time. Si samples must be handled as little as possible; only 40 minutes of light irradiation is required for sample cleaning. Samples should be prepared with 0.1 M glycolide and 0.001 M Sn(Oct)<sub>2</sub>, although the order of addition is of little importance. Some stirring (ca. 100 RPM) is beneficial but should not be excessive (ca. 300 RPM is too high). Finally, the recrystallization solvent used for monomer purification plays an important role in the production of reproducible brush growth. The thickest brushes were obtained when using a recrystallization solvent whose boiling point was very close to, but not above the melting point of the monomer.

### **3.5. Experimental Details**

#### **3.5.1. Si chip preparation**

Silicon substrates were cut in to 1.5 cm × 2.0 cm pieces from 4.0” silicon wafers with [100] orientation (Wafer World, Inc.). Once dried the Si samples were placed in Ultra-Violet Ozonolysis, UVO instrument for 40 minutes unless noted otherwise. Cleaned Si chips were

measured via ellipsometry (for initial thickness) and then taken to the dry box for polymer brush sample preparation.

### **3.5.2. Polymer bush growth preparation**

Tin(II) ethyl-hexanoate ( $\text{Sn}(\text{Oct})_2$ ) was used as a catalyst for polymer brush growth. The final catalyst concentration was 0.001 M unless noted otherwise. Glycolide was slowly added to each sample vial (5 mL of 0.1 M monomer in THF unless noted otherwise). Sample vials were sealed tightly with Teflon caps. Prepared samples were then taken to an incubated environment to ensure constant temperature (28 °C) and rotation speed (100 RPM) unless otherwise noted.

### **3.5.3. Reaction quenching**

After the specified reaction time had been reached, samples were removed from the reaction environment, placed in 5 mL anhydrous tetrahydrofuran, THF, and sonicated for 15 s. Following sonication, polymer brush samples were rinsed with an excess of DI water and ethanol then dried under a stream of gaseous nitrogen. Dried samples were measured via ellipsometry for a final polymer brush thicknesses. Samples were stored in sterile Petri dishes under ambient conditions.

#### **3.5.4. Distilled or recrystallized monomers and solvents**

Glycolide (mp. 86-88 °C) was recrystallized twice. Once with anhydrous ethyl acetate (bp. 77.1 °C) followed by anhydrous acetonitrile (bp. 82 °C). Crystals were dried via vacuum filtration under a stream of gaseous nitrogen. Semi-dry crystals were further dried under reduced pressure (ca. 5 mTorr) for 48 h at 35 °C.

THF was distilled from sodium, benzophenone. Anhydrous THF was collected in an oven dried (nitrogen cooled) side-arm receiver flask. Ethyl acetate, acetone and acetonitrile were distilled at their respective boiling points.

The monomer and solvents were stored in a nitrogen atmosphere (dry box) sealed with Teflon fitted caps. The THF was further tested for dryness in the drybox after collection. The tests were carried out by adding 10 µL of a previously prepared mixture of sodium and benzophenone to 10 mL of solvent.

#### **3.5.5. Ellipsometry**

Sample thicknesses were measured by a single-wavelength ellipsometer at a 70° angle (AutoEL-III, Rudolph Research, Flanders, USA). All measurements were taken on dry samples. Five measurements, four at the corners and one at the center, were taken on each sample. Measurements were taken before and after brush growth in order to obtain a more accurate ellipsometric thickness.

### 3.5.6. Glassware

20 mL reaction vials (with Teflon lids) were used throughout the polymer brush experiments. For cleaning, the vials were soaked in toluene, followed by base bath solution (isopropyl alcohol and KOH). After thorough scrubbing, the vials were rinsed with DI water and acetone respectively. Vials were purged with nitrogen gas. All glassware was used hot from overnight drying ca. 130 °C.

### 3.6. References

1. Xu, L.; and Gorman, C. B., Poly(lactic acid) Brushes Grow Longer at Lower Temperatures. *J. Poly. Sci.: Part A: Poly. Chem.* **2010** *48*, 3362–3367.
2. Turgman-Cohen, S.; Genzer, J., Computer Simulation of Controlled Radical Polymerization: Effect of Chain Confinement Due to Initiator Grafting Density and Solvent Quality and “Grafting From” Method. *Macromol.* **2010**, *43*, 9567-9577.
3. Black, L. E.; McIntosh, K. R., Defect Generation at Charge-Passivated Si-SiO<sub>2</sub> Interfaces by Ultraviolet Light. *IEEE Transactions on Electron Devices* **2010**, *8*, 1996-2004.
4. Kowalski, A.; Duda, A.; Penczek, S., Kinetics and Mechanism of Cyclic Esters Polymerization Initiated with Tin(II) Octoate. 3. Polymerization of *L,L*-Dilactide. *Macromol.* **2000**, *33*, 7359-7370.
5. Wigal, C., Purifying Acetanilide by Recrystallization. In *Modular Laboratory Program in Chemistry*, Neidig, H. A., Chemical Education Resources: Palmyra, PA, **1997**; pp 1-12.

## Chapter 4: Poly(glycolic acid) and Poly( $\epsilon$ -caprolactone) Brush Degradation: Preliminary Results

### 4.1. Introduction

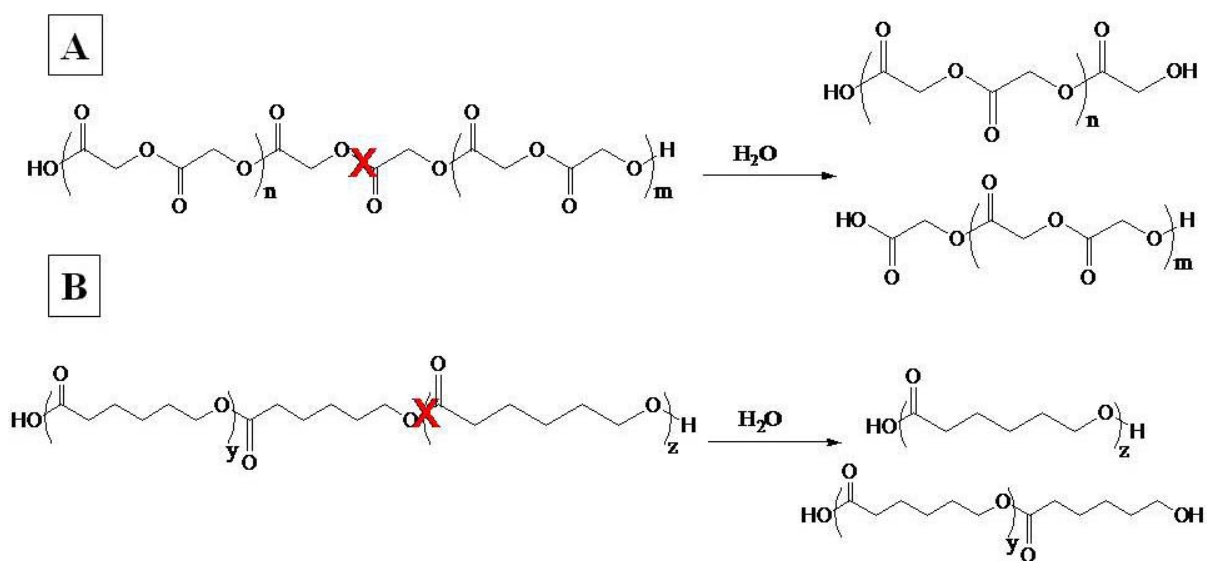
The growth of poly(glycolic acid) (PGA) and poly( $\epsilon$ -caprolactone) (PCL) brushes have been discussed in the previous chapters. Here, attention is focused on their degradation. Although considerable progress has been made toward the full characterization of bulk polyester degradation, there is scant reporting that describes the behavior of hydrolysis for biodegradable polyesters of PGA and PCL brushes on a surface. When considering bulk PGA and PCL, literature reports suggest that the rate of hydrolysis is highly dependent on the environmental conditions to which the polymer is exposed (i.e. solvent, reaction temperature and pH).<sup>1,2</sup> In addition, contributions such as glass transition temperature, concentration, density and crystallinity play a significant role in determining the length of time required for the degradation of PGA and PCL.<sup>3,4</sup> As a result of these contributing factors, complete hydrolysis of the bulk polyesters can take from days to weeks or longer to occur.<sup>4</sup>

When considering PGA and PCL brushes, the relative rates of degradation are hypothesized to be different from the bulk polymer for at least two reasons. First, polymer brushes only have one available terminal chain end. If hydrolysis takes place at the chain end(s), then this can be a factor in the rate of degradation. Second, the molecular weight,  $M_n$ , of a polymer chain on a brush is very small when compared to the  $M_n$  of a polymer chain in solution. Reports have shown that oligomers with a relatively small  $M_n$  degrade differently

than bulk polymer;<sup>5</sup> this may also be the case for brushes. These differences will likely have a significant effect on the relative rates of degradation for PGA and PCL brushes.

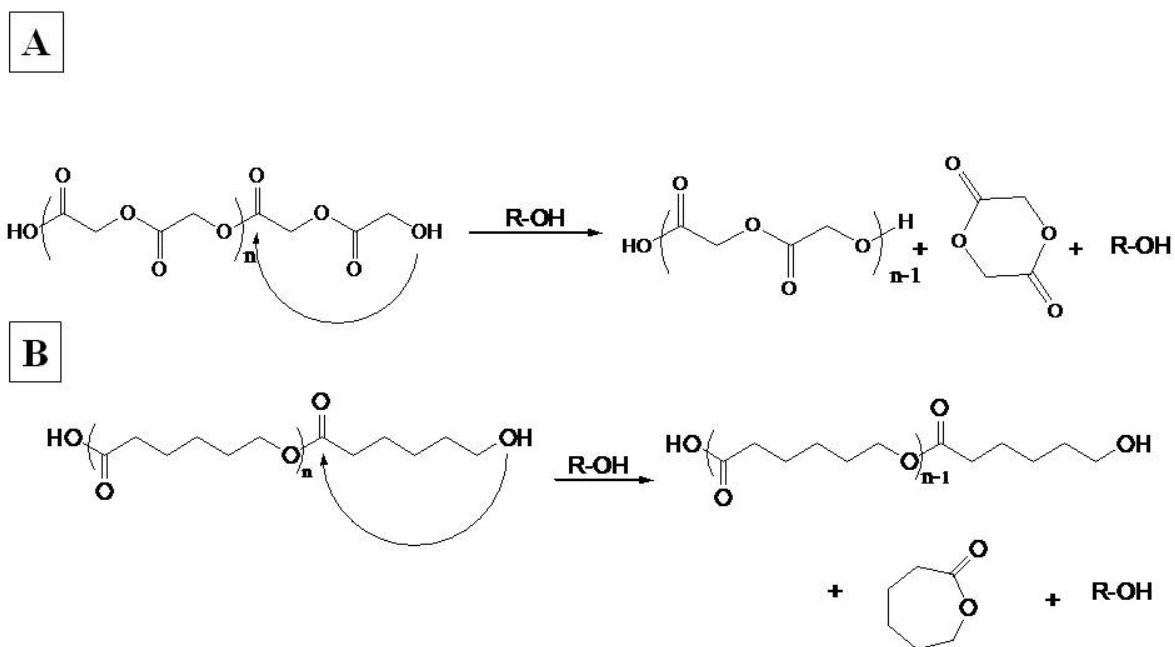
The biodegradation of polyesters is thought to occur through one of two mechanisms. The first is through random chain scission of the ester bonds along the polymer chain (Scheme 4.4). Random chain scission is said to be partially dependent on the rate of solvent diffusion into the polymer matrix. For a bulk polymer, the rate of solvent diffusion is affected by the polymers' structure and its inherent degree of crystallinity.<sup>5</sup>

Scheme 4.4: Proposed random chain scission mechanism for hydrolysis of PGA (A) and PCL (B).



The second mechanism is through intramolecular transesterification commonly referred to as back-biting (Scheme 4.5).<sup>6,7</sup> A computational study has shown that chain end scission via back-biting has occurs more rapidly than random chain scission.<sup>8,9</sup> Although schemes of the degradation mechanisms have been provided as a visual aid, the exact mechanism(s) by which degradation occurs is complex. Factors such as molecule mobility, solvent type and local pH also play an important role in the degradation mechanism(s).<sup>8</sup>

Scheme 4.5: Proposed backbiting mechanism for the hydrolysis of PGA (A) and PCL (B).



A recent report by our group looked into the effects of temperature and pH on the degradation of PLA brushes and suggested a likely mechanism by which degradation occurs.<sup>10</sup> A summary of the work completed is provided here. PLA brushes of ca. 10 nm were placed in phosphate buffer (PB) pH 7.4 (10 mM ionic strength) at 25 °C, 37 °C and 60 °C. Their ellipsometric thicknesses were measured and plotted as a function of time; the corresponding plot has been reproduced in Figure 4.22. PLA brushes were found to degrade more quickly at elevated temperatures. Degradation at 25 °C was complete after ca. 375 h while the degradation at 37 °C and 60 °C occurred after only ca. 100 h and 20 h respectively. Increasing the temperature by only 12 °C increased the rate of degradation by a factor of 4.<sup>10</sup>

## PLA Brush Degradation by Xu et al.

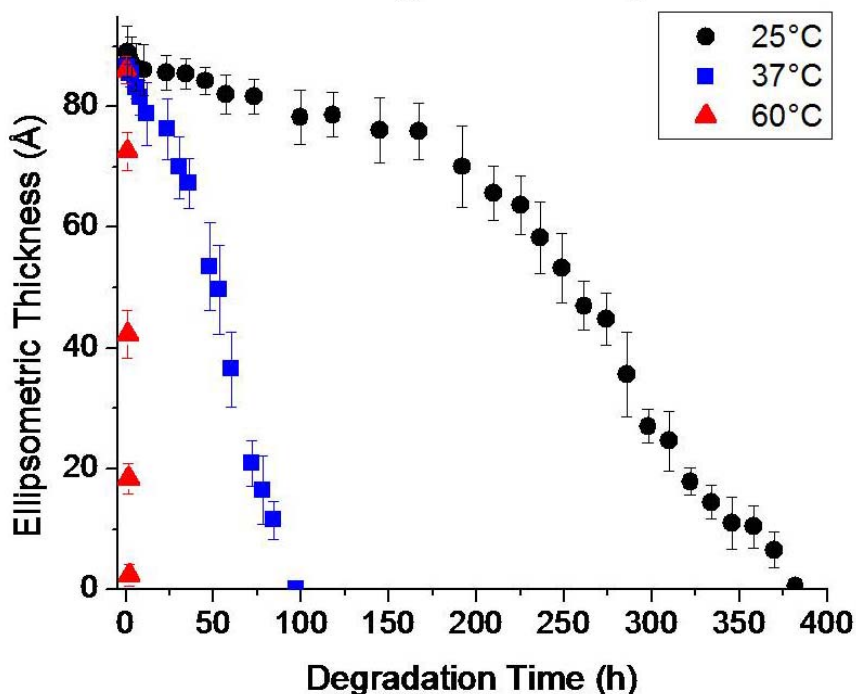


Figure 4.22: Plots of ellipsometric thicknesses versus degradation time at different temperatures. Phosphate buffer pH = 7.4 with 10 mM ionic strength used to control pH. Error bars represent the magnitude of the 90% confidence interval for 5 measurements on a sample.

In a separate experiment from the same report, PLA brushes of ca. 10 nm thickness were placed in different PB solutions at 37 °C (10 mM ionic strength) with pH values 3.0, 6.0, 7.0, 7.4 and 8.0. Their ellipsometric thicknesses were measured as a function of time for a period of 400 h; the corresponding plot has been reproduced in Figure 4.23. PLA brushes at pH 3.0 and 6.0 did not degrade on this time scale. However, the rate of degradation increased greatly at pH values greater than 6.0. Complete degradation for pH 7.0, 7.4 and 8.0 occurred after ca. 375 h, 110 h and 24 h respectively.

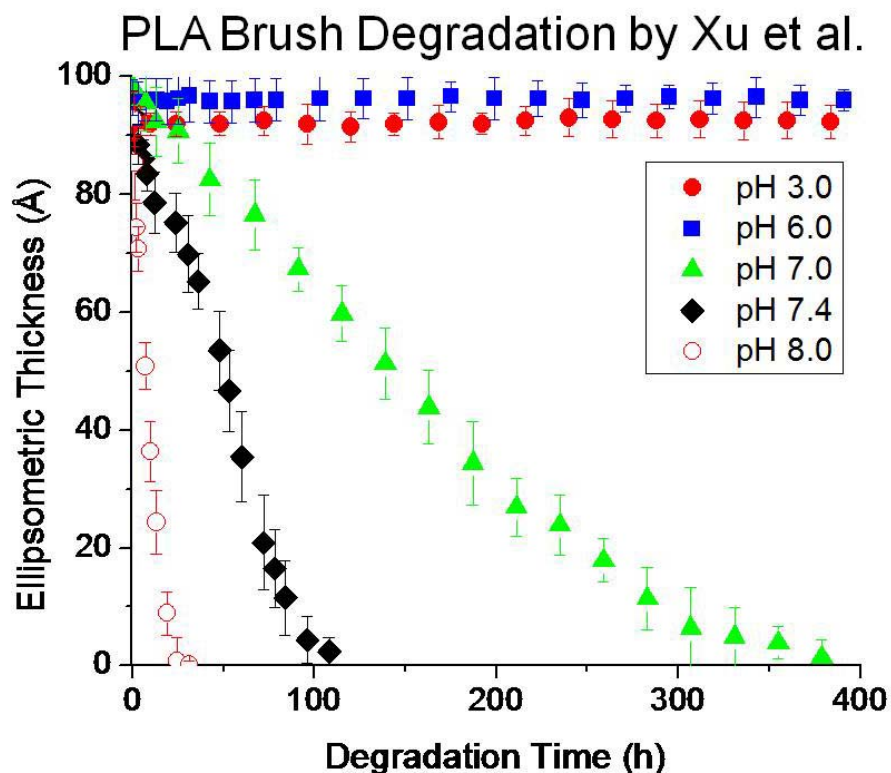


Figure 4.23: Plots of ellipsometric thicknesses versus degradation time at 37 °C with different pH values. Phosphate buffers of 10 mM ionic strength were used to control pH. Error bars represent the magnitude of the 90% confidence interval for 5 measurements on a sample.

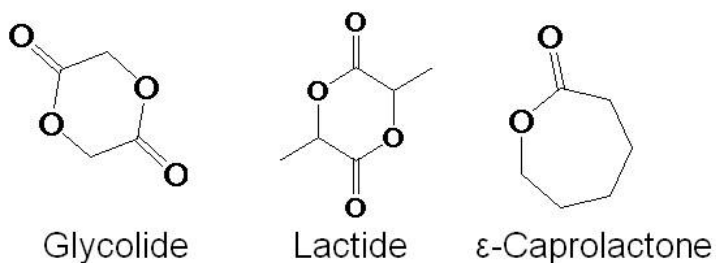
Hydrolysis of PLA brushes at elevated pH likely occurs via intramolecular transesterification (back-biting). This claim is based, in part, on findings reported by de Jong and van Nostrum for their work on the degradation of PLA oligomers.<sup>5,8</sup> In aqueous solution Xu and Gorman produced evidence that polymer brushes with terminal hydroxyl groups orient/reorient themselves so that they are present at the surface/solution interface. When removed from aqueous solution the terminus hydroxyl groups bury themselves within the brush. The change in surface wettability was followed using deionized water contact angle

measurements. The results correspond well with literature reports.<sup>11,12</sup> For PLA brushes in basic solution, the terminal end of the polymer chain is likely to play a critical role in back-biting.<sup>13</sup> Hydrolysis via intramolecular transesterification would result in the original, closed ring monomer and a polymer chain that is two lactic acid units shorter. Back-biting would continue until complete degradation has occurred. Furthermore, the cyclic monomers are subsequently susceptible to hydrolysis.

It is of interest to apply similar degradation conditions to PGA and PCL brushes in effort to determine their relative rates of degradation. Based on the structural similarity between the L-lactide and glycolide monomers (Scheme 4.6), it is likely that their corresponding polyester brush degradation trends would also be similar. However, when comparing monomers L-lactide and  $\epsilon$ -caprolactone, it is anticipated that brush degradation for PCL brushes will be slower than for PLA brushes under the same conditions. The anticipated, slower degradation of PCL is based on two key factors. First, bulk PCL is more hydrophobic than PLA which may slow the rate of solvation in aqueous solution. Second, compared to PLA, PCL has fewer ester linkages for a given mass which will likely decrease the probability for hydrolysis to occur.<sup>14</sup> In support of this, literature has shown that the hydrolysis of bulk PCL is much slower compared to the hydrolysis bulk PLA under the same conditions. Lam et al. reported bulk PCL scaffolds to have lost 86% of the original mass after 41 months of hydrolysis under physiological conditions.<sup>15</sup> In contrast, Grizzi et al. reported bulk PLA devices to have lost 90% of the original weight after only 13 weeks under physiological conditions.<sup>16</sup> Here, preliminary work on the rate of degradation for PGA and

PCL brushes was investigated and are compared with the rates of degradation for PLA brushes.

Scheme 4.6: Molecular structures of glycolide, lactide and  $\epsilon$ -caprolactone.



## 4.2. Results and Discussion

### 4.2.1. Reproducing poly(lactic acid) brush degradation

Degradation of a PLA brush with ca. 10 nm ellipsometric thickness was carried out using pH 7.4 PB (10 mM ionic strength) at 37 °C; these conditions are analogous to biological environments. The decrease in brush thickness was followed via ellipsometry and was plotted as a function of time. The results are compared with PLA brush degradation reported by previous group member, Xu (Figure 4.24).<sup>10</sup> For the current experiment, the time required for complete brush removal was ca. 110 h. The initial difference in degradation rate (0-24 hours) is likely attributed to the removal of physisorbed polymeric residue before exposing the PLA brush for degradation.

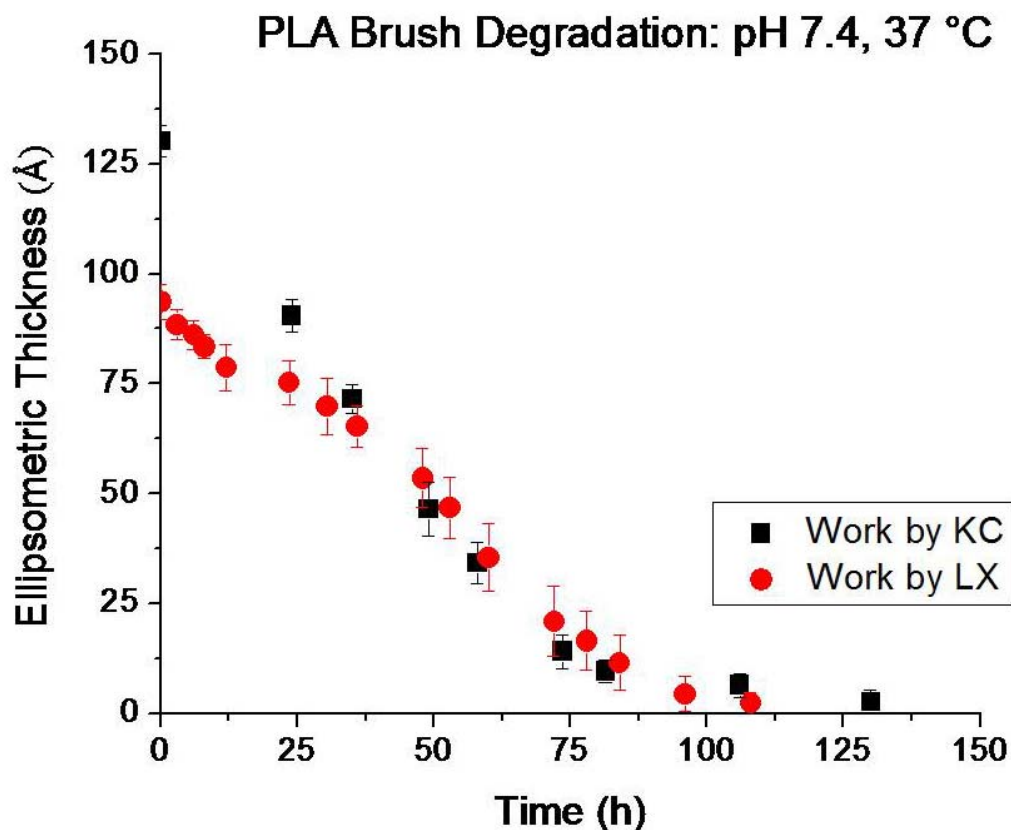


Figure 4.24: Plots of ellipsometric thicknesses versus degradation time for PLA brushes. Reaction conditions: phosphate buffer (10 mM ionic strength), pH 7.4 at 37 °C. Error bars represent the magnitude of the 90% confidence interval for 5 measurements on a sample.

#### 4.2.2. Poly(glycolic acid) brush degradation

A PGA brush of ca. 12 nm thickness was incubated at 37 °C in pH 7.4 phosphate buffer solution (10 mM ionic strength). The change in brush thickness was measured via ellipsometry and was plotted as a function of time (Figure 4.25). Complete removal of the grafted PGA brush (ca. 12 nm) from the sample surface occurred after ca. 140 h. The

relative rate of PGA brush degradation is similar to the degradation of PLA brushes<sup>10</sup>; this can be seen in Figure 4.25.

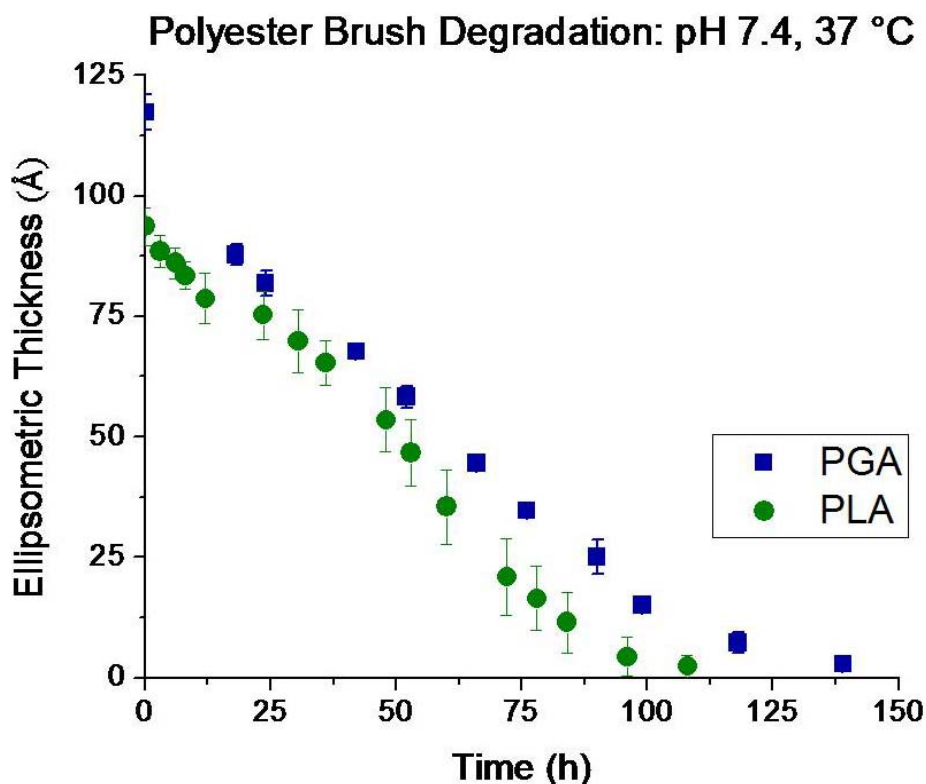


Figure 4.25: Plots of ellipsometric thicknesses versus degradation time comparing a PGA and PLA brush. Reaction conditions: phosphate buffer (10 mM ionic strength), pH 7.4 at 37 °C. Error bars represent the magnitude of the 90% confidence interval for 5 measurements on a sample.

#### **4.2.3. Poly( $\epsilon$ -caprolactone) brush degradation**

PCL brushes of ca. 8 nm thickness were exposed to aqueous solutions of phosphate buffer (10 mM ionic strength) at pH 3.0 or pH 8.0. The samples were incubated at 37 °C throughout the experiments. Changes in brush thickness were measured via ellipsometry and were plotted as a function of time (Figure 4.26). At pH 3.0, no degradation occurred after ca. 750 h (1 month). Instead, a slight increase in ellipsometric thickness occurred through the first 100 h; this is likely attributed to physisorption of material in the buffer solution. In an effort to avoid physisorption the sample solution was changed daily (after 100 h). Following this change the brush thickness remained constant for the remainder of the experiment.

Initially at pH 8.0, neither an increase nor decrease in thickness was observed after the same 100 h period. Thus, the basic buffer solution was also changed daily after 100 h. Following the change in reaction conditions the sample at pH 8.0 steadily decreased until complete removal of polymer was achieved (after ca. 650 h).

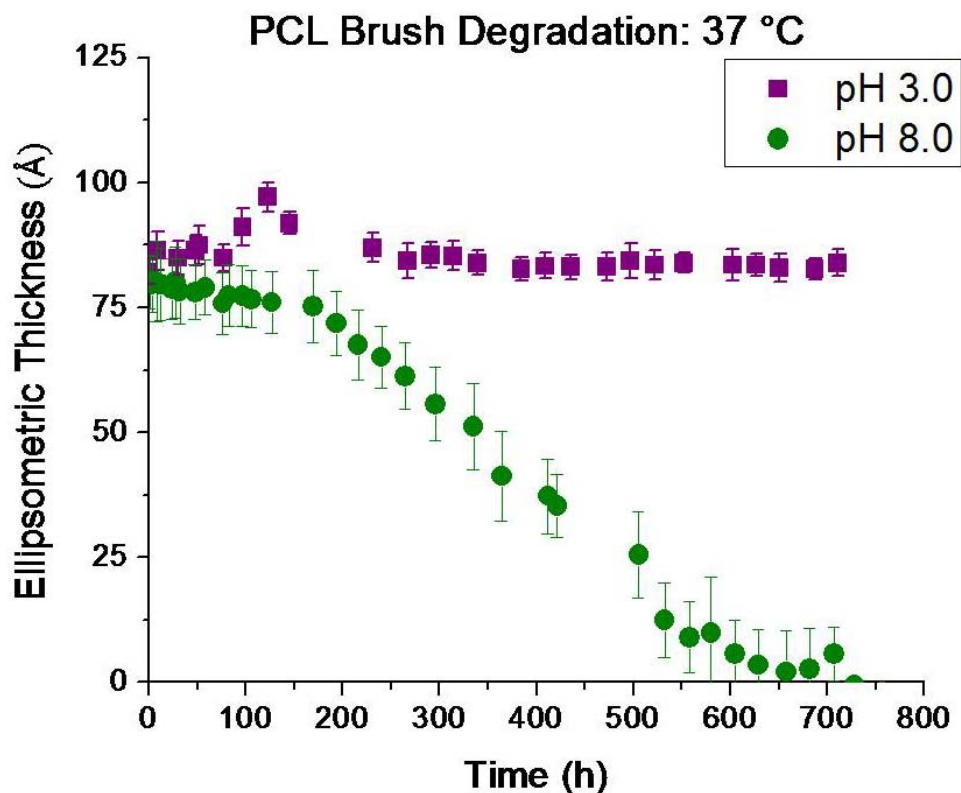


Figure 4.26: Plots of ellipsometric thicknesses versus degradation time for PCL brushes. Reaction conditions: phosphate buffer (10 mM ionic strength), 37 °C, changed sample solution daily after ca. 110 h. Error bars represent the magnitude of the 90% confidence interval for 5 measurements on a sample.

Degradation of PCL brushes occurred slowly in basic media and not at all under acidic conditions during the time scale of the experiment (1 month). Though the general trend of degradation is similar to the degradation of PLA brushes, the relative rates of degradation in basic solutions are quite different. Recall that PLA brushes with ca. 10 nm thickness completely degraded in pH 8.0 phosphate buffer (10 mM ionic strength) at 37 °C after 24 h. In contrast, when exposed to the same conditions, albeit with a lower, initial

ellipsometric thickness (8 nm), PCL brush degradation was significantly slower requiring nearly a month to reach complete removal from the silicon surface.

As previously suggested, there are two key factors that played a likely role in the slower degradation of PCL brushes. First, PCL is more hydrophobic than PLA and thus is more capable of resisting solvent diffusion into the polymer matrix when exposed to aqueous solutions. Second, compared to PLA, PCL has fewer ester linkages for a given mass which likely decreases the probability for hydrolysis to occur.<sup>14</sup> The combination of these two structural differences accounts for the slower PCL brush degradation.

### **4.3. Conclusion**

Polymer brush degradation was monitored for PLA, PGA and PCL brushes. The brushes for PLA were degraded using procedures presented by a previous group member, Lebo Xu. PGA brush hydrolysis occurred at nearly the same rate in pH 7.4 PB (10 mM ionic strength) at 37 °C when compared to PLA brush degradation under the same conditions.

Brushes for PCL degraded more slowly in pH 8.0 PB (10 mM ionic strength) at 37 °C when compared to PLA brush degradation under the same conditions. As previously discussed (above), the likely causes for slower PCL hydrolysis (when compared to PLA) can be attributed to the increased hydrophobicity of PCL as well as the presence of fewer ester bonds for a given mass of polymer, providing fewer sites available for hydrolysis to occur.<sup>14</sup> PCL brushes did not degrade under acidic conditions (pH 3.0, PB with 10 mM ionic strength,

37 °C) during the time scale of the experiment. The preliminary results obtained from this work showed that degradation does occur for PGA and PCL brushes under basic conditions. The data provided for the relative rates of PGA and PCL brush degradation will prove beneficial for the further advancement of temporary protective coatings.

#### **4.4. Proposal for Future Work**

The growth and hydrolytic degradation of PGA and PCL brushes were investigated and discussed in this thesis. As a result of the research completed, some extensions of this project are proposed here. Provided that the proper conditions can be determined to establish reproducible PCL brush growth (see Chapter 2) studies on the degradation of PGA and PCL would be particularly interesting to follow when exposed to protein containing environments. Research studies dedicated to the development of biocompatible surfaces of this nature are already under way and would serve as a good reference point.<sup>17,18</sup>

A few adjustments to the synthesis/degradation of PGA and PCL may be worthwhile to consider in effort to prepare for experiments that are more biologically focused. To start, brushes should be grown from gold surfaces instead of silicon surfaces. When tracking polymer brush degradation from gold substrates, additional characterization methods can be used such as, cyclic voltammetry (CV) and quartz crystal microbalance with dissipation (QCM-D). The formation of polyester brushes grown from gold substrates can be achieved by using a hydroxyl terminated self-assembled monolayers (SAMs) on gold as an initiator.<sup>10</sup>

Moreover, reports have shown that the use of SAM initiators provide better control over the initiator surface coverage and subsequently the grafting density.<sup>19</sup>

For CV, the magnitude of the oxidation and reduction peaks of an electroactive species in solution (i.e. ferricyanide) can be followed for brush degradation or protein adsorption. As the PGA or PCL brushes degrade, an increase in current should be seen – or as proteins adsorb on the brush surface a decrease in current may (or may not) be observed. CV experiments that follow brush degradation are currently being investigated by another group member for PLA brushes. QCM-D can be used to follow the same experiments discussed for CV but can also be employed to follow brush growth.<sup>20,21</sup>

By using CV and or QCM-D to track polymer brush degradation or protein absorption, important information can be gained regarding the biocompatibility of the PGA and PCL brushes. If required, further improvement of biocompatibility for the PGA and PCL brushes may be obtained by incorporating other polymers. The synthesis of random or co-block brushes formed by using a combination of the two polymers or by incorporating other polymer such as poly(ethylene oxide) or PLA may help to improve their use in medical devices. Similar studies have already been reported and may aid in the further development for the synthesis and characterization of these brushes.<sup>22,23</sup>

## **4.5. Experimental Details**

### **4.5.1. Polymer brush degradation**

Polymer brush samples were placed in 20 mL reaction vials with 10 mL of phosphate buffer solution (10 mM ionic strength). pH values of 3.0, 7.4 and 8.0 were established with the addition of phosphoric acid (98%) or sodium hydroxide. After a designated length of time samples were removed from the buffer solution, rinsed with excess DI H<sub>2</sub>O and ethanol and dried under a stream of gaseous nitrogen for ellipsometric measurements. Samples were immediately returned to the buffered solution following ellipsometry characterization.

### **4.5.2. Ellipsometry**

Sample thicknesses were measured by a single-wavelength ellipsometer at a 70° angle (AutoEL-III, Rudolph Research, Flanders, USA). All measurements were taken on dry samples. Five measurements, four at the corners and one at the center, were taken on each sample. Measurements were taken before and after brush growth in order to obtain a more accurate ellipsometric thickness.

### **4.5.3. Glassware**

20 mL reaction vials (with Teflon lids) were used throughout the polymer brush experiments. For cleaning, the vials were sonicated in toluene, followed by base bath solution (isopropyl alcohol and KOH). The cleaned vials were rinsed with water, DI water and acetone respectively. All glassware was oven dried overnight at 130 °C prior to use.

## 4.6. References

1. Li, S.; McCarthy, S., Further Investigations on the Hydrolytic Degradation of Poly(DL-lactide). *Biomaterials* **1999**, *20*, 35-44.
2. Gilding, D. K.; Reed, A. M., Biodegradable Polymers for Use in Surgery-Polyglycolic/Poly(actic acid) Homo- and Copolymers: 1. *Polymer* **1979**, *20*, 1459-1464.
3. Jung, J. H.; Ree, M.; Kim, H., Acid- and Base-Catalyzed Hydrolyses of Aliphatic Polycarbonates and Polyesters. *Catal. Today* **2006**, *115*, 283-287.
4. Siparsky, G. L., Degradation Kinetics of Poly(hydroxy) Acids: PLA and PCL. In *Polymers from Renewable Resources Biopolyesters and Biocatalysis*, Carmen Scholz, R. A. G., Ed. American Chemical Society: Washington, DC, 2000; pp 230-251.
5. de Jong, S. J.; Arias, E. R.; Rijkers, D. T. S.; van Nostrum, C. F.; Kettenes-van den Bosch, J. J.; Hennink, W. E., New Insights into the Hydrolytic Degradation of Poly(lactic acid): Participation of the Alcohol Terminus. *Polymer* **2001**, *42*, 2795-2802.
6. Labet, M.; Thielemans, W., Synthesis of Polycaprolactone: A Review. *Chem. Soc. Rev.* **2009**, *38*, 3484-3504.
7. Zurita, R.; Franco, L.; Puiggali, J.; Rodriguez-Galan, A., They Hydrolytic Degradation of a Segmented Glycolide-Trmethylene Carbonate Copolymer (Maxon<sup>®</sup>). *Polym. Degrad. Stab.* **2007**, *92*, 975-985.
8. van Nostrum, C. F.; Veldhuis, T. F. J.; Bos, G. W.; Hennink, W. E., Hydrolytic Degradation of (Oligo)lactic acid): a Kinetic and Mechanistic Study. *Polymer* **2004**, *45*, 6779-6787.
9. Batycky, R. P.; Hanes, J.; Langer, R.; Edwards, D. A., A Theoretical Model of Erosion and Macromolecular Drug Release from Biodegrading Microspheres. *J. Pharm. Sci.* **1997**, *86*, 1464-1467.
10. Xu, L.; Crawford, K.; Gorman, C. B., Effects of Temperature and pH on the Degradation of Poly(lactic acid) Brushes. *Macromol.* **2011**, *44*, 4777-82.

11. Wallace, W. E.; Fischer, D. A.; Efimenko, K.; Wu, W.-L.; Polymer Chain Relaxation: Surfaces Outspaces Bulk. Genzer, J. *Macromol.* **2001**, *34*, 5081–5082.
12. Holmes-Farley, S. R.; Reamey, R. H.; Nuzzo, R.; McCarthy, T. J.; Whitesides, G. M., Reconstruction of the Interface of Oxidatively Functionalized Polyethylene and Derivatives on Heating. *Langmuir* **1987**, *3*, 799–815.
13. Lee, S. H.; Kim, S. H.; Han, Y. K.; Kim, Y. H., Synthesis and Degradation of End-Group-Functionalized Polylactide. *J. Polym. Sci.: A, Polym. Chem.* **2001**, *39*, 973-985.
14. Lee, W. K.; Gardella, J. A., Hydrolytic Kinetics of Biodegradable Polyester Monolayers. *Langmuir* **2000**, *16*, 3401-3406.
15. Lam, C. X. F.; Savalani, M. M.; Teoh, S. H.; Hutmacher, D. W., Dynamics of in vitro Polymer Degradation of Polycaprolactone-based Scaffolds: Accelerated versus Simulated Physiological Conditions. *Biomed. Mater.* **2008**, *3*, 034108.
16. Grizzi, I.; Garreau, H.; Li, S.; Vert, M., Hydrolytic Degradation of Devices Based on Poly(DL-lactic acid) Size-Dependence. *Biomaterials* **1995**, *16*, 305-311.
17. Mendes, P., Stimuli-Responsive Surfaces for Bio-Applications. *Chem. Soc. Rev.* **2008**, *37*, 2512-2529.
18. Ares, N., Polymer Brushes: Applications in Biomaterials and Nanotechnology. *Polym. Chem.* **2010**, *1*, 769-777.
19. Zhao, B.; Brittain, W. J., Polymer Brushes: Surface-Immobilized Macromolecules. *Prog. Polym. Sci.* **2000**, *25*, 677-710.
20. Chen, X. A.; Zhang, Y. Z.; He, J. A.; Xiong, C. Y.; Meng, Y. H.; Jin, G.; Ma, H. W., Quartz Crystal Microbalance study of the Kinetics of Surface Initiated Polymerization. *Sci. China Ser. B- Chem.*, **2009**, *52*, 2307-2322.
21. Moya, S. E.; Brown, A. A.; Azzaroni, O.; Huck, W. T. S., Following Polymer Brush Growth Using the Quartz Crystal Microbalance Technique. *Macromol. Rapid Commun.* **2005**, *26*, 1117-1121.

22. Mao, J.; Gan, Z., Amphiphilic PEG-co-PGL-g-PCL Copolymer Brushes: Synthesis, Micellization and Controlled Drug Delivery. *Macromol. Chem. Phys.* **2009**, *210*, 2078-2086.
23. Zhang, W.; Li, Y.; Liu, L.; Sun, Q.; Xhuai, X.; Zhu, W.; Chen, Y., Amphiphilic Toothbrushlike Copolymers Based on Poly(ethylene glycol) and Poly( $\epsilon$ -caprolactone) as Drug Carriers with Enhanced Properties. *Biomacromol.* **2010**, *11*, 1331-1338.